THE EFFECT OF PRESSURE ON HUMIDIFICATION AND DEHUMIDIFICATION PROCESSES FOR HDH DESALINATION SYSTEMS

BY

HUICHENG LIU

A Thesis Presented to the
DEANSHIP OF GRADUATE STUDIES

KING FAHD UNIVERSITY OF PETROLEUM & MINERALS

DHAHRAN, SAUDI ARABIA

In Partial Fulfillment of the
Requirements for the Degree of

MASTER OF SCIENCE

In

MECHANICAL ENGINEERING

MAY 2015

KING FAHD UNIVERSITY OF PETROLEUM & MINERALS

DHAHRAN- 31261, SAUDI ARABIA

DEANSHIP OF GRADUATE STUDIES

This thesis, written by **HUICHENG LIU** under the direction his thesis advisor and approved by his thesis committee, has been presented and accepted by the Dean of Graduate Studies, in partial fulfillment of the requirements for the degree of **MASTER OF SCIENCE IN MECHANICAL ENGINEERING.**

Dr. Mostafa H. Sharqawy
(Advisor)

Dr. Zuhair M. Gasem
Department Chairman

Dr. Mohamed A. Antar
(Member)

Dr. Salam A. Zummo
Dean of Graduate Studies

Dr. Syed M. Zubair
(Member)

11/6/15

Date

DEANSHIP OF GRADUATE STUDIES

Dedicated To My Beloved Family

For their endless love, support and encouragement

ACKNOWLEDGMENTS

I feel grateful to be enrolled at King Fahd University of Petroleum and Minerals two years ago, and have an honor today to accomplish this thesis work successfully for partial completion of M.S. degree in Mechanical Engineering. Owing to this precious opportunity, I must express my whole thanks to a list of people whom I will keep forever in mind and cherish deep in heart.

My sincere gratitude and appreciation belong to my thesis advisor and mentor Dr. Mostafa H. Sharqawy for his professional instruction, continuous motivation and merciful attitude. I was armed with the valuable knowledge he gave, and realized more unknown in the science world demands to be explored. I was energized with the persistent endeavor he had, and believed personal effort deserves along the lifetime. I am also greatly indebted to Dr. Mohamed A. Antar and Dr. Syed M. Zubair. I was always feeling welcome and encouraged whenever I sought their favor. Many thanks for their valuable time spent and supportive suggestions provided. I consider myself lucky for having the brilliant and amiable professors as my thesis committee members.

I am thankful to all of my admirable instructors at KFUPM. The high-level education enriched my post-graduate studies and will benefit me in my career. Special thanks to the staff in the laboratory and workshop, their generous assistances contribute to my experimental work. I equally appreciate the wonderful friends I met during my graduate study for their kind help and interesting sharing. Once more, acknowledgment is due to KFUPM for offering full scholarship and financial support, and funding the research

reported in this thesis through National Science, Technology and Innovation Plan office, NSTIP Project # 11-WAT1625-04.

I would like to have great thanks to my parents, for their all-weather care and support. I enjoyed sharing my overseas life and making joy with them, but also used to convey the pressure, difficulty and complaint to them. Whatever I did, they would listen, understand, comfort and encourage me and eventually helped me to be better man. And I would also like to thank my younger sister, for her cheering me up magically every time. Frankly, the flying time cannot degrade the gratitude to the former teachers and mentors in my homeland either, for their fundamental cultivation and superior responsibility. Also constant thanks to my old friends and classmates, as friendship always being.

Thanks to all, the warm people, the pretty nature… in earnest.

TABLE OF CONTENTS

ACKNOWLEDGMENTS v

TABLE OF CONTENTS vii

LIST OF FIGURES x

NOMENCLATURE xiii

ABSTRACT xvi

ملخص الرسالة xviii

CHAPTER 1 INTRODUCTION 1

1.1 HDH Desalination Technology 1

1.2 Bubble Columns 5

1.3 The Effect of Pressure 15

1.4 Objectives and Outline of the Thesis 18

CHAPTER 2 BUBBLE COLUMN DEHUMIDIFIER 20

2.1 Mathematical Model 20

2.1.1 Dehumidifier at Constant T_c 20

2.1.2 Dehumidifier at Constant T_{wi} 32

2.2 Experimental Work 38

2.2.1 Dehumidifier at Constant T_c 38

2.2.2 Dehumidifier at Constant T_{wi} 43

2.3 Results and Discussion 49

2.3.1 Dehumidifier at Constant T_c 49

2.3.2 Dehumidifier at Constant T_{wi} 58

2.4 Chapter Conclusions 67

CHAPTER 3 BUBBLE COLUMN HUMIDIFIER 69

3.1 Mathematical Model 69

3.2 Experimental Work 75

3.2.1 Experimental Setup 75

3.2.2 Experimental Procedure 78

3.2.3 Calibration and Uncertainty Analysis 80

3.3 Results and Discussion 81

3.3.1 The Air and Water Outlet Temperatures 81

3.3.2 Effect of Column Liquid Height 84

3.3.3 Effect of Superficial Velocity 86

3.3.4 Effect of Pressure 89

3.3.5 The Use of ε–*NTU* Model 90

3.4 Chapter Conclusions 92

CHAPTER 4 CONCLUSIONS AND RECOMMENDATIONS 93

4.1 Conclusions 93

4.2 Recommendations 95

REFERENCES 96

VITAE 100

LIST OF FIGURES

Figure 1-1 Basic water-heated HDH desalination system with closed air loop and open water loop 4

Figure 1-2 Schematic of experimental apparatus with the air path indicated [20].....8

Figure 1-3 Schematic of evaporation chamber with air pipe, electrical water heater and external graduate level (H is measured as the static water height before the experimental test, ΔH is the effective water height during the experimental test) [13].....10

Figure 1-4 Schematic of bubble column dehumidifier used by [11].....12

Figure 1-5 Schematic of the inclined evaporator chamber merged with solar collector [25] 14

Figure 1-6 Effect of pressure on the humidity ratio of saturated moist air.....16

Figure 2-1 Schematic of a bubble column dehumidifier 21

Figure 2-2 (a) Temperature and humidity ratio gradients inside a bubble; (b) Thermal resistance network.....22

Figure 2-3 Schematic of the bubble column with a finite volume element 23

Figure 2-4 Schematic of the bubble column dehumidifier at constant T_{wi} 33

Figure 2-5 A finite volume element in a bubble column dehumidifier with a counter flow configuration.....34

Figure 2-6 Photo of the bubble column dehumidifier 38

Figure 2-7 Schematic of the laboratory scale test-rig for dehumidifier test at fixed T_c ... .39

Figure 2-8 Schematic of the experimental setup for dehumidifier test at fixed T_{wi} 44

Figure 2-9 Photo of the laboratory scale test-rig without showing the compressor and vacuum pump 45

Figure 2-10 Air exit temperature from the dehumidifier at different pressures and superficial velocities 50

Figure 2-11 Effect of the bubble column initial water height on the total heat transfer rate 52

Figure 2-12 Effect of bubble column initial water height on the effectiveness 52

Figure 2-13 Empirical correlation of Sherwood number with other dimensionless groups 53

Figure 2-14 Effect of the superficial velocity and the pressure on the total heat transfer rate, the lines indicate the model predictions 55

Figure 2-15 Effect of the superficial velocity and the pressure on the effectiveness, the lines indicate the model predictions 56

Figure 2-16 A comparison between the predicated and the measured heat transfer rates 56

Figure 2-17 Effectiveness vs. *NTU* at various pressures and superficial velocities 57

Figure 2-18 Outlet temperatures of air (a) and water (b) in the bubble column dehumidifier at different pressures and superficial velocities 59

Figure 2-19 Effect of the static water column height on the total heat transfer rate (a) and effectiveness (b) in the bubble column dehumidifier 61

Figure 2-20 Effect of the superficial velocity and the pressure on the total heat transfer rate (a) and effectiveness (b) in the dehumidifier 63

Figure 2-21 Effect of the superficial velocity and the pressure on the mass transfer coefficient in the dehumidifier 65

Figure 2-22 Experimental values of the effectiveness and *NTU* for the dehumidifier plotted with their corresponding model values given by Equation (2-36) ..66

Figure 3-1 Schematic of the bubble column humidifier at constant T_{wi} 70

Figure 3-2 A finite volume element in a bubble column humidifier with a counter flow configuration 71

Figure 3-3 Schematic of the experimental setup for humidifier test at fixed T_{wi} 77

Figure 3-4 Outlet temperatures of air (a) and water (b) in the bubble column humidifier at different pressures and superficial velocities 83

Figure 3-5 Effect of static water column height on the total heat transfer rate (a) and effectiveness (b) in the bubble column humidifier..... 85

Figure 3-6 Effect of the superficial velocity and the pressure on the total heat transfer rate (a) and effectiveness (b) in the humidifier 87

Figure 3-7 Effect of the superficial velocity and the pressure on the mass transfer coefficient in the humidifier..... 88

Figure 3-8 Experimental values of the effectiveness and *NTU* for the humidifier plotted with their corresponding model values given by Equation (3-10)..... 91

NOMENCLATURE

Symbols

a	specific area (surface area per unit volume)	m^{-1}
A_c	cross-sectional area of bubble column	m^2
c_p	specific heat at constant pressure	J/(kg·K)
D	diffusion coefficient	m^2/s
d_b	bubble diameter	m
d_o	perforated plate orifices diameter	m
g	gravitational acceleration	m/s^2
h	convective heat transfer coefficient	$W/(m^2 \cdot K)$
h_d	convective mass transfer coefficient	$kg/(m^2 \cdot s)$
H	height	m
i	specific enthalpy	J/kg
i_{fg}	enthalpy of vaporization	J/kg
$\dot{m}$	mass flow rate	kg/s
$n_{0\text{-}3}$	correlation coefficients in Eq. (2-17)	—
P	pressure	Pa
$\dot{q}$	rate of heat transfer	W
R	thermal resistance	K/W
T	temperature	°C
$\dot{V}$	volumetric flow rate	m^3/s
V	volume	m^3
V_g	superficial velocity	m/s

z	coordinate	—

Greek Symbols

ϵ	gas holdup	—
ε	effectiveness	—
μ	dynamic viscosity	kg/(m·s)
ρ	Density	kg/m^3
σ	surface tension	N/m
ω	humidity ratio	$kg_{vapor}/kg_{dry\text{-}air}$

Subscripts

a	air
c	liquid in bubble column
c1	initial liquid height
c2	aerated liquid height
da	dry air
f	saturated liquid
g	saturated vapor
i	inlet
lat	latent
m	measured
o	outlet
r	ratio
s	saturated
sc	saturated air at column liquid temperature

sen	sensible
v	water vapor
w	water inside the coil

Dimensionless groups

GOR	Gain Output Ratio	—
HCR	Heat Capacity Ratio	—
Le_f	Lewis factor	$h/(h_d c_{pa})$
NTU	Number of Transfer Units	$(h_d a V_c)/\dot{m}_a$
Re	Reynolds number	$(\rho_a V_g d_b)/\mu_a$
Sc	Schmidt number	$\mu_a/(\rho_a D)$
Sh	Sherwood number	$(h_d d_b)/(\rho_v D)$

ABSTRACT

Full Name: Huicheng Liu

Thesis Title: The Effect of Pressure on Humidification and Dehumidification Processes for HDH Desalination Systems

Major Field: Mechanical Engineering

Date of Degree: May 2015

Variable pressure humidification dehumidification desalination (HDH) system was regarded in the literature as an efficient HDH process compared with a single pressure one. This thesis investigates theoretically and experimentally the effect of pressure on the humidification and dehumidification processes for HDH application. Since it is not practical to build conventional humidifier or dehumidifier at sub-atmospheric or elevated pressures, bubble column humidifier and dehumidifier are used as a practical alternative. The experimental investigation comprises of three test cases: (1) bubble column dehumidifier at elevated pressures and constant column temperature; (2) bubble column dehumidifier at elevated pressures and constant inlet water temperature; (3) bubble column humidifier at sub-atmospheric pressures and constant inlet water temperature. The bubble columns examined are of 10 cm diameter and 25 cm height, equipped with internal cooling and heating coils, and air is sparged through perforated plates at their bottoms. The elevated pressure in the dehumidifier ranges from 15 – 30 psia, while the reduced pressure in the humidifier ranges from 7 – 15 psia. In addition, the water level in the bubble columns and the superficial velocity were varied in the range of 3 – 7 cm and 2 – 20 cm/s respectively. The performance was evaluated by measuring the total heat transfer rate and the effectiveness. Moreover, the experimental values of the mass transfer

coefficient are presented as a function of the superficial velocity and pressure. A model is developed for the relationship between the bubble column effectiveness (ε) and the number of transfer units (NTU) which combines the influence of the heat and mass transfer processes. In addition, a semi-empirical model is adopted and modified for the gas-side mass transfer coefficient to capture the effect of the pressure. The model correlates Sherwood number with Reynolds number, Schmidt number, and the density ratio of air and water vapor.

The proposed ε -NTU model is found to agree well with the experimental results. The results show that the sub-atmospheric pressure promotes the humidifier performance as a consequence of increasing heat transfer coefficient and effectiveness. However, the elevated pressure is not beneficial for the dehumidifier effectiveness, although the heat transfer rate is slightly increased. In addition, it was found that the liquid height in the bubble column has no effect on the heat transfer in the range of the heights examined. However, the superficial velocity was found to have a significant effect on both the humidifier and dehumidifier thermal performance due to the turbulence increase. Therefore, it is recommended to operate a bubble column humidifier under sub-atmospheric pressure, but the bubble column dehumidifier which is operated under elevated pressure requires a larger component size to overcome the lower effectiveness.

ملخص الرسالة

الاسم الكامل: هوشينج ليو

عنوان الرسالة: تأثير الضغط على عمليات الترطيب والتجفيف فى أنظمة تحلية المياه بالـ HDH

التخصص: الهندسة الميكانيكية

تاريخ الدرجة العلمية: مايو 2015

نشرت بعض الابحاث مؤخرا عن ان نظام تحليه المياة بالترطيب والتجفيف الذى يعمل تحت ضغوط متغيرة يعتبر اكثر كفاءة من نظيره الذى يعمل عند ضغط جوى. هذه الأطروحة تبحث نظريا وتجريبيا تأثير الضغط على عمليات الترطيب والتجفيف. وحيث انه ليس عمليا بناء مرطب او مجفف تقليدي يعمل عند ضغوط منخفضه أو مرتفعة، لذلك تم استخدام عمود الفقاعات كبديل عملى للمرطب و المجفف والذى يمكنه العمل عند ضغوط متغيره. وتشتمل الاختبارات العملية على ثلاث حالات: (1) عمود فقاعى مجفف العمود يعمل عند ضغوط مرتفعة ودرجة حرارة عمود ثابت؛ (2) عمود فقاعى مجفف يعمل عند ضغوط مرتفعة ودرجة حرارة مياه داخله ثابتة. (3) عمود فقاعى مرطبيعمل عند ضغوط منخفضة ودرجة حرارة مياه داخله ثابته. والأعمدة المفحوصة قطرها 10 سم وارتفاعها 25 سم ومجهزة بملفات تبريد وتدفئة ويتم دخول الهواء من خلال لوحات مثقوبة عند القاع. والضغط المرتفع في المجفف يتراوح من 15-30 رطل، في حين أن الضغط المنخفض المرطب يتراوح من 7-15 رطل. بالإضافة إلى ذلك، تم تغيير منسوب المياه في الأعمدة وكذلك سرعة الهواء في حدود 3-7 سم و2-20 سم / ثانية على التوالي. تم تقييم الأداء من خلال قياس معدل انتقال الحرارة والفاعلية. وعلاوة على ذلك، تم تطوير نموذج رياضى للعلاقة بين فعالية العمود وعدد وحدات النقل الذي يجمع بين تأثير عمليتى انتقال الحرارة والكتلة. بالإضافة إلى ذلك، تم اعتماد نموذج شبه تجريبي وتعديله للتنبؤ بمعامل انتقال الكتلة تحت تأثير الضغط حيث يربط هذا النموذج بين رقم شيروود مع رقم رينولدز، ورقم شميدت ونسبة كثافة الهواء الى بخار الماء.

اظهرت النتائج ان النموذج المقترح للفاعلية وعدد وحدات النقل تتوافق جيدا مع النتائج التجريبية. كما أظهرت النتائج أن انخفاض الضغط يعزز من أداء المرطب نتيجة لزيادة معامل انتقال الحرارة والفاعلية. ولكن وجد إن ارتفاع الضغط لا يفيد من فاعلية المجفف، على الرغم من أن معدل انتقال الحرارة يزيد بشكل طفيف. وبالإضافة إلى ذلك،

فقد وجد أن ارتفاع السائل في العمود ليس له أي تأثير على انتقال الحرارة في حدود الارتفعات التى تم فحصها. ومع ذلك، وجد ان زيادة سرعة الهواء له تأثير كبير على اداء كل من المرطب والمجفف نتيجة زيادة الاضطراب. ولذلك، فمن المستحسن أن تعمل المرطبات عند ضغط منخفض، ولكن لا ينصح بعمل المجفف تحت ضغط مرتفع لما يتطلبه حجم أكبر للتغلب على نقص الفاعلية.

CHAPTER 1

INTRODUCTION

1.1 HDH Desalination Technology

Desalination is a process which produces fresh water from saline or brackish water. It is a reliable, economic and sustainable technical solution to the global water scarcity. With the increasing demand of fresh water in remote communities, a number of small-scale desalination systems have been investigated specifically for its energy efficiency, economic feasibility, and environmental aspects. Humidification–Dehumidification (HDH) desalination technology is a thermal desalination process which is adaptable for small or large scale fresh water production. HDH process is based on the principle of humidifying a gas by saline water then dehumidifying it at a lower temperature. The fresh water is the condensate resulting from the dehumidification process. The HDH system is composed mainly of a humidifier, a dehumidifier, and a heater for heating either the carrier gas or the water (see Figure 1-1). The efficiency of the HDH desalination system depends mainly on the performance of the humidifier and dehumidifier.

The major components in the HDH system are the humidifier and dehumidifier. In the humidifier, the entering dry air directly contacts with hot water and carries water vapor from it. The concentration (or humidity ratio) difference between the water vapor carried by the air and the water-air interface drives the water diffusion into the moist air in the form of latent heat transfer. The temperature difference between the air and the water

streams results in the heat transfer from water to the air in form of sensible heat transfer. The temperature increase of the moist air promotes its water vapor carrying capacity. In the dehumidifier, the hot moist air contacts with the cold water and transfers some water vapor content to the contact surface with distilled water generation. The principle in the dehumidifier is analogous but opposite to that of the dehumidifier. The saturated (usually) air releases sensible and latent heat loads in results of temperature and humidity ratio decreases. Simultaneously, the water in the dehumidifier is preheated by the heat transfer from the hot-humid air. The dehumidifier recovers the vaporized water and latent heat of evaporation by condensation.

Convectional humidifier and dehumidifier such as packed-bed and finned-tube heat exchanger have been investigated in previous studies [1–3]. These equipment have very low heat and mass transfer coefficients and require large volume; hence, high capital cost. For instance, in packed-bed humidifiers, the specific surface area of the mass transfer process (surface-area-to-volume ratio) depends on the type of the fill which is either film or splash type, constructed or unconstructed packing. In all types the specific surface area is very low which requires large packing volume. Narayan et al. [4] reviewed different packing materials (such as wood, plastic, honeycomb paper, etc.) used in HDH systems. The heat and mass transfer performance, efficiency and durability are some aspects to be considered for this equipment. The high fouling impact is also a typical problem needs careful attention.

On the other hand, various types of heat exchangers can be used as dehumidifiers. The finned-tube heat exchanger is frequently used as a dehumidifier component in HDH systems [5–7]. However, finned-tube heat exchanger dehumidifiers have very low condensation heat transfer coefficient of the air–vapor mixture due to the large amount of non-condensable gases. This requires large surface area of tubes and fins which consequently increase pressure drop inside the tubes and on the gas side. In addition, scale formation on the outside surface of the tubes and fouling inside the tubes are considered major issues in finned tube heat exchanger, in particular when working with saline water. Yamali and Solmus [6] designed three parallel dehumidifiers in an integrated and insulated metal box to avoid leakage of distilled water. The internal body of the dehumidifier box is manufactured with copper tubes connected with corrugated aluminum fins. The packed tower as a direct contact dehumidifier was first used in the HDH system by Khedr [8], but the thermal performance is limited due to low energy recovery.

There are three categories of HDH systems which depend on: (1) the source of the energy supply (e.g. thermal, electric, solar, geothermal, or hybrid sources); (2) the heated stream (e.g. water-heated and air-heated system); (3) cycle configuration (including closed-water open-air (CWOA) and closed-air open-water (CAOW)). Based on these categories, various configurations and arrangements especially for some novel types were developed in the published literature. Chafik [9] proposed a multi stage solar air heating HDH systems where each heating stage stepped by a humidification stage. The continuous heating and humidification processes with make-up seawater can maintain the humid air temperature in a range of 50 – 80 °C, and achieve a high humidity ratio of

0.093 $kg_{vapor}/kg_{dry\text{-}air}$ after four stages. Müller-Holst [10] investigated a multi-effect HDH system which enables continuous temperature stratification in the evaporation and condensation process, by which the energy afforded in the humidifier is mostly regained in the dehumidifier and hence a high energy recovery and efficiency is achieved.

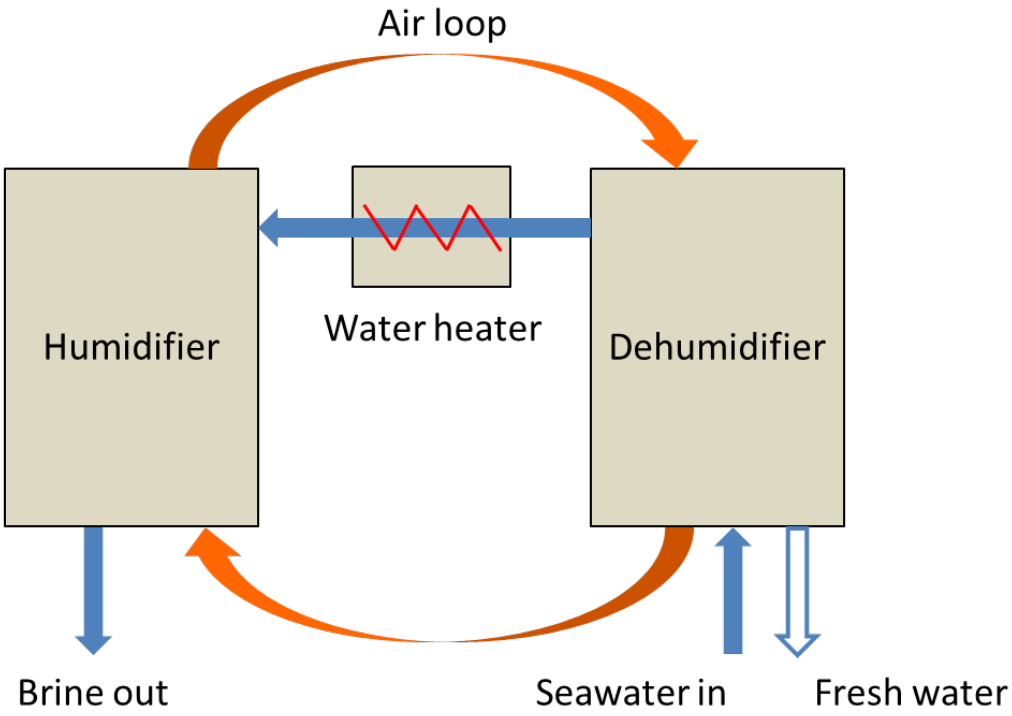

Figure 1-1 Basic water-heated HDH desalination system with closed air loop and open water loop

1.2 Bubble Columns

Bubble column reactor is a device where a gas is sparged in the form of bubbles into a column of liquid or a liquid–solid mixture. They are considered as multiphase reactors wherein simultaneous heat and mass transfer occurs between the gas bubbles and the liquid in the column. Recently, some investigators [11–14] proposed to use bubble columns in humidification dehumidification (HDH) desalination systems. In the HDH process, hot-humid air leaves a humidifier almost saturated with water vapor, and then the water vapor condenses and releases its latent heat in a dehumidifier. Bubble columns could be used in HDH systems as humidifiers, dehumidifiers, or both since they have great advantages of reducing the size required for humidification or dehumidification process due to the large contact area and the low thermal resistances [11,12].

As a multiphase device, bubble column reactor has complex flow dynamics and thermo-physical characteristics which attract considerable interests of investigations. The design parameters of bubble column include its geometry, sparger design, and internals, subject to the operating variables such as flow rate, temperature, and pressure. Bubble columns are typically designed in vertical cylindrical shapes. The column diameter ranges from 0.1 m to 0.5 m for a typical experimental scale, whereas larger column diameter from 1 m to 10 m with length (or height)-to-diameter ratio at least 5 is commonly employed in industrial applications [15,16]. There are numerous categories of bubble column reactors which depends on their configurations, commonly formed with sieve trays, packed, multi-shaft and static mixers in spite of the simplest form without any internals [17]. In addition, there are different types of gas sparger (or distributor) in

bubble column reactors. Reported in the publication of Kantarci et al. [15], they are generally categorized into three items: ring type, arm distributor and perforated plate. Highly effective gas distribution can be obtained in perforated plate but the range of gas flow rate should be considered.

Determined by the superficial velocity at a given bubble column geometry, the flow regimes in the bubble columns can be subdivided into four patterns: homogeneous (bubbly), heterogeneous (churn-turbulent and slug), and annular flow [15,18]. The industrial bubble columns are usually operated at the heterogeneous bubble flow regime. In homogeneous flow regime, the bubbles have uniform size and shape, while they are distributed in heterogeneous flow regime. The difference in flow characteristics between different flow regimes affects significantly the heat and mass transfer rates [18]. For a given bubble column, the homogeneous flow regime takes place in a low superficial velocity, and heterogeneous flow regime results in a high superficial gas velocity. Although some experiments and models have been conducted on the detection of various flow regimes, there still lack of a comprehensive regime map for various conditions. Besides, it is important to mention that these flow regimes are applied only to bubble columns of high aspect ratios (height-to-diameter ratio > 5). Tow and Lienhard [19] recently investigated shallow bubble columns (aspect ratio of 0.025 – 0.425) and concluded that they may have no region of developed flow.

Some attentions are now paid to bubble columns to be utilized as humidifiers and dehumidifiers in HDH desalination system. In bubble columns, the carrier gas is dispersed into a liquid column to form small bubbles instead of direct contact with solid surface. The enormous number of small bubbles results in a large interfacial surface area

and enhanced heat and mass transfer processes hence small equipment volume. There are few studies which proposed using bubble columns in HDH desalination systems. Vlachogiannis et al. [20] studied an HDH system which uses a combination of bubbles generation and mechanical vapor compression. In their experimental apparatus shown in Figure 1-2, air is dispersed as bubbles through a porous plate at the bottom of a saline water column in an evaporation chamber where it is humidified. The exit humid air flows to a compressor where it is pressurized and heated. Then, the air flows through an air distributor connected to 25 vertical tubes where condensation occurs on the internal surface of the tubes. After that, the air flows back to the evaporation chamber to form a closed-loop air cycle. Their experimental measurements show that increasing the saline water temperature will increase the fresh water production and decrease the compressor energy consumption.

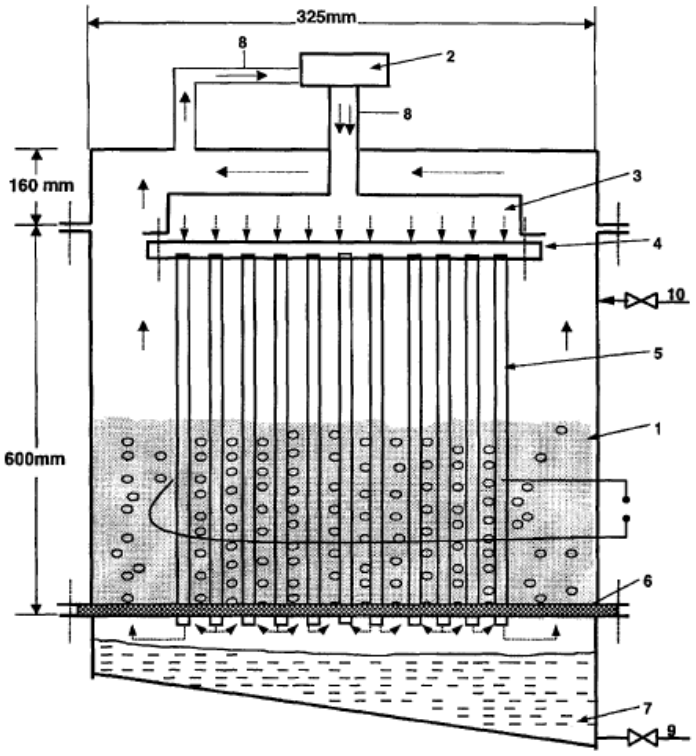

Figure 1-2 Schematic of experimental apparatus with the air path indicated [20]

(1) saline water, (2) compressor, (3) air distributor, (4) tube sheet, (5) tubes, (6) porous wall, (7) fresh water, (8) K-thermocouples, (9) outlet manual valve, (10) filling manual valve

El-Agouz and Abugderah [13] investigated experimentally the performance of a bubble column humidification process. The performance was evaluated by measuring the humidification efficiency (defined as the actual difference of the humidity ratio to the maximum difference) under varying operating conditions. An air supply pipe with 32 holes of 10 mm diameter each was submerged into the hot water column of an evaporation chamber (see Figure 1-3). The results showed that, the humidification efficiency increases with the increase of the water column temperature, air inlet temperature, and the air velocity. El-Agouz [14] further investigated a complete HDH system which was mainly equipped with an air compressor, two shell-and-tube heat exchangers served as a dehumidifier, and a bubble column humidifier. The bubble column humidifier had a 40×30 cm^2 cross-sectional area and 125 cm height where air enters through a perforated pipe drilled with 44 holes of 15 mm diameter each. The measurements were conducted under air flow rate up to 14 kg/hr (equivalent to a superficial velocity of 2.8 cm/s), water temperature in the range of 50 – 90 °C, and water column height in the range of 20 – 60 cm. It was found that both of the humidifier efficiency and the fresh water productivity increase with the air flow rate and water temperature, but are slightly affected by the water column height.

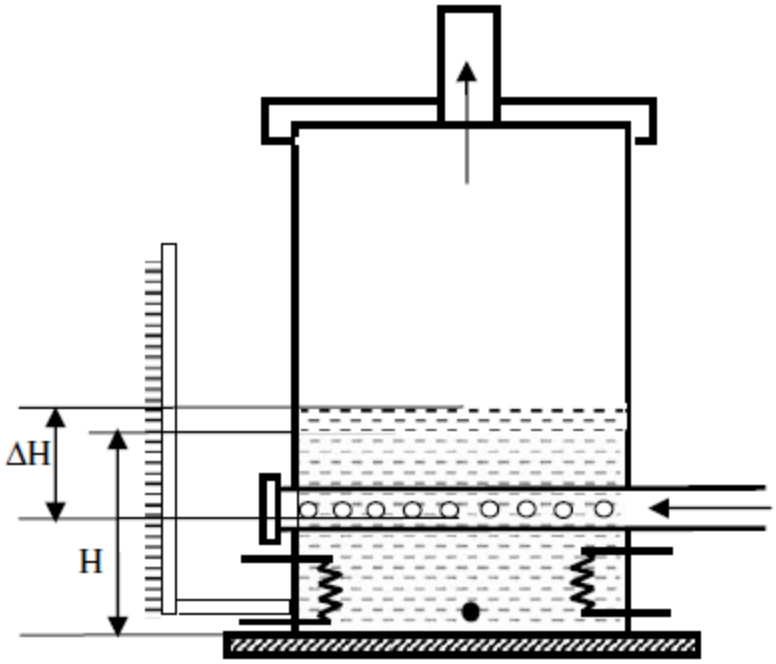

Figure 1-3 Schematic of evaporation chamber with air pipe, electrical water heater and external graduate level (*H* is measured as the static water height before the experimental test, *ΔH* is the effective water height during the experimental test) [13]

Bubble column has also been applied in the dehumidification process of HDH desalination system. In a bubble column dehumidifier, vapor carried by the air bubbles condenses on the interfacial area between the bubble surface and the cold liquid film in the column. The latent heat of vaporization is released from the air–vapor mixture to the fresh water. Different from the saline water allowed in the humidifier, the liquid in the dehumidifier bubble column must be filled with fresh water for the sake of condensation mixing. The cold source can be obtained from an indirect contact with coolant fluid (saline water or other liquids), which is separated with fresh water by a cooling coil immersed in the bubble column. Narayan et al. [11] presented a theoretical and experimental investigation of bubble column dehumidifier. They conducted experiments on two bubble columns made of polyvinyl chloride (PVC), and in dimensions of approximately 300 mm × 300 mm cross-sectional area and 460 mm height for each. The operating conditions vary in a superficial velocity range of 4 – 8 cm/s and a bubble diameter range of 4 – 6 mm. One of the bubble columns was used as a humidifier, where the supplied air was passed through a perforated plate upward into hot water. The other one was used as a dehumidifier with similar perforated plate where hot-humid air was passed through a cold water column. The liquid in the humidifier is directly heated by an electrical heater, while the cold source in the dehumidifier is provided by the coolant flow in the copper coil. As shown in Figure 1-4, the bubbles were generated by supplying hot air through a porous plate into a cold water column. The cooling load was provided by the chilled water inside the cooling coil. Theoretically, Narayan et al. [11] developed a thermal resistance model which involved some remarkable thermal resistances associated with the different temperatures. They proposed and determined the sensible and latent

heat resistances for the heat and mass transfer between the entering air and the liquid in the column. In addition, they considered the thermal resistances inside and outside the cooling coil due to convection heat transfer. To estimate the mass transfer coefficient at the air side and the liquid side of the bubble–liquid interface, they referred to the theory of surface renewal constructed by Higbie [21] and derived an expression for the surface renewal time (or contact time) by assuming a characteristic length and velocity scale. The sensible heat from the air side to the liquid side is modeled by the Logarithmic Mean Temperature Difference (LMTD) method. Their results showed that high superficial velocity and low bubble diameter are favorable to the heat transfer while the column height has no effect on the total heat transfer. The measured heat transfer rates were performed higher than those obtained in existing state-of-the-art dehumidifiers by an order of magnitude.

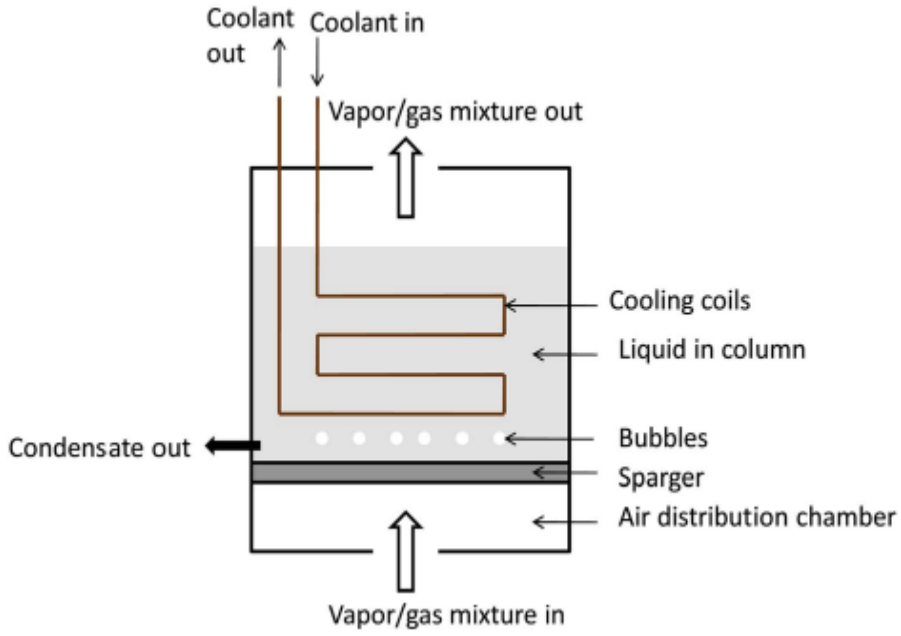

Figure 1-4 Schematic of bubble column dehumidifier used by [11]

A similar investigation was conducted by Tow and Lienhard [12], but they further simplified the thermal network model proposed by Narayan et al. [11] by neglecting the gas-side thermal resistance. They assumed that the thermal resistance inside the air bubbles should be regarded as zero under perfect mixing conditions [22]. Their modified thermal resistance model included only the heat transfers inside and outside the cooling coil. The convection heat transfer coefficient inside the coil was calculated based on the correction for laminar flow in curved tubes [23], and the heat transfer coefficient outside the coil was calculated using Deckwer's correlation [24] for gas-liquid dispersion to immersed coil. Tow and Lienhard [12] investigated the performance of a bubble column dehumidifier of 28 × 28 cm^2 area and 36 cm height and has a perforated plate and copper coil internally installed. For air flow rate in the range of 1.5 – 2.5 L/s (equivalent to superficial velocity of 1.9 – 3.2 cm/s), the heat flux increases almost linearly with the air flow rate. Moreover, parallel-flow effectiveness was proposed as the ratio of the actual heat transfer rate to the maximum heat transfer rate assuming the outlet temperatures of air and water streams equal to the column liquid temperature. Using their effectiveness definition, they demonstrated that the effectiveness decreases with the air flow rate (or superficial velocity). On the other hand, it was found that the effectiveness is independent on the column liquid height if it is higher than 4 cm.

Bubble columns could contain a heating or a cooling coil to provide the heat needed for the humidification process or extract the heat released from the dehumidification process. Different from this configuration, Ghazal et al. [25] presented a bubble column humidifier combined with a flat-plate solar collector where the solar collector was filled with water and air was sparged from a copper pipe at its bottom (see Figure 1-5). The

copper pipe had a diameter of 1.3 cm, a length of 60 cm, and many holes of 2 mm diameter on its side. It was found that the relative humidity of exit air is nearly 100% and the humidification efficiency (based on absolute humidity ratio) is above 90%. It was demonstrated that the direct contact system of air–water bubble column is feasible and efficient for the humidification process.

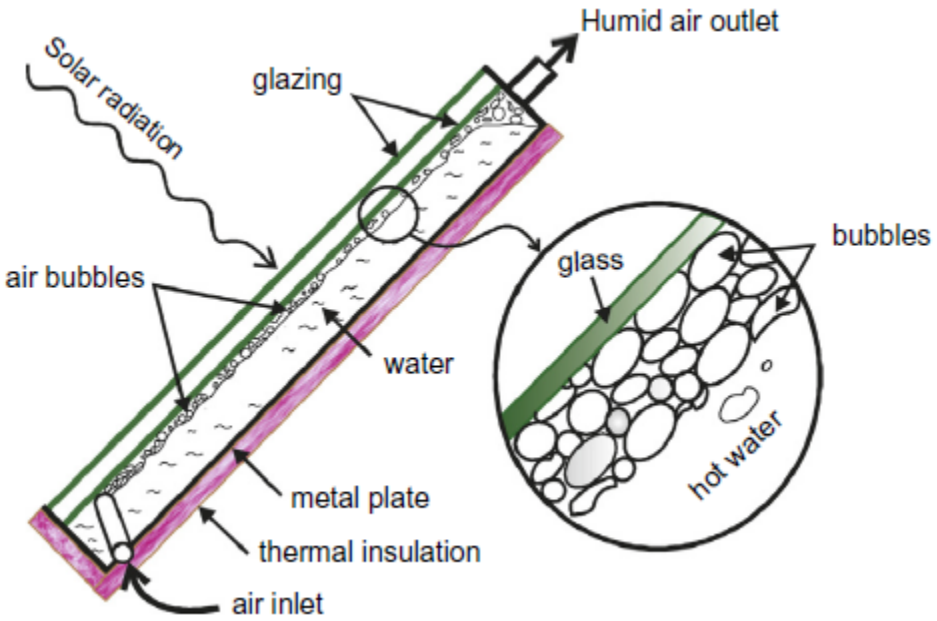

Figure 1-5 Schematic of the inclined evaporator chamber merged with solar collector [25]

1.3 The Effect of Pressure

The operating conditions of the HDH system such as mass flow rates, temperature, pressure, and effectiveness of the humidifier and dehumidifier; have great impact on the overall performance of the system and the gain output ratio (*GOR*) which is the enthalpy of vaporization of the produced fresh water per unit energy added. It was demonstrated by Narayan et al. [26] that the HDH system performance could be improved if it works under variable pressure condition. This means that the humidifier works at sub-atmospheric pressure while the dehumidifier works at elevated pressure. The psychometric analysis (see Figure 1-6) showed that the capacity of the moist air to carry water vapor increases when the humidification process occurs at sub-atmospheric pressure. On the other hand, the condensation of the water vapor in the dehumidifier will be improved if it operates at elevated pressure. Consequently, the fresh water production is increased and the *GOR* of the HDH system is improved.

Ghalawand et al. [27] studied theoretically a variable pressure HDH system with a packed-bed humidifier working at 1 bar and a flash drum dehumidifier working at 3 bar. A compressor was used to increase the pressure and temperature of the humid air after the humidifier and a throttling valve was used to reduce the pressure after the dehumidifier in a closed-air cycle. The value of *GOR* was calculated to be 2.07. Higher *GOR* (> 1) indicates that the HDH system working under elevated dehumidifier pressure is efficient.

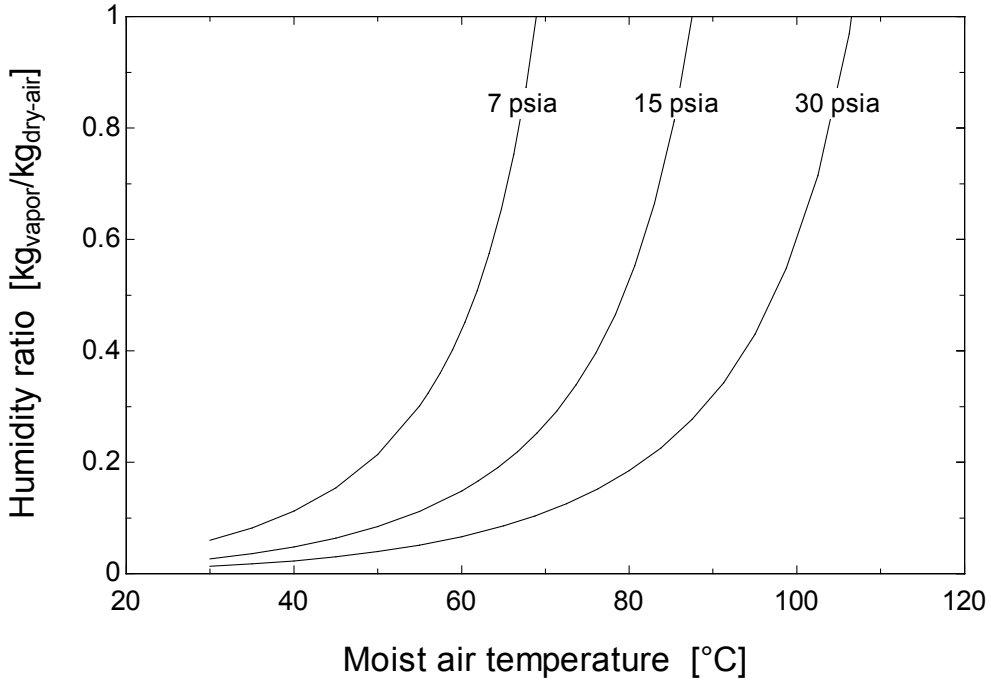

Figure 1-6 Effect of pressure on the humidity ratio of saturated moist air

It should be noted that, the advantages of varying pressure on the HDH system in preceding statements are only ideally suits for a basic and complete cycle regardless of which component types being used and what other performance parameters response to the varying pressure. In practice, different types of humidifier and dehumidifier could achieve various performances under varying pressure. The pressure has complicated effects on the overall system performance. As previously introduced as a promising humidifier and dehumidifier component, bubble column is usually operated at non-atmospheric conditions in industrial applications [28]. However, almost all HDH systems utilizing bubble column [11–14] were experimentally investigated at atmospheric pressure. Therefore, an investigation of the pressure effect on the performance of bubble column reactors is desired.

A review by Kantarci et al. [15] showed that increasing the pressure in bubble columns has a positive effect on both the bubble characteristics and the thermodynamic performance. Letzel et al. [29] measured the gas holdup of nitrogen–water system in a bubble column of 15 cm diameter and 1.22 m height operated at a pressure range of 0.1 – 1.3 MPa. Their experimental results indicated that the gas holdup almost double when the pressure increases from 0.1 to 1.3 MPa. Increasing pressure directly leads to the increase of the gas density and the decrease of the bubble diameter. Consequently, the mass transfer coefficient increases with the increase of the gas density and pressure as reported by many researchers [28–32]. The effect of pressure on the heat transfer coefficient has also been investigated but is still inconclusive. For example, Wu et al. [33] found that the heat transfer coefficient in an air–water bubble column decreases at higher pressures up to 10 bar. However, other experimental measurements indicated that the heat transfer

coefficient increases with the pressure [34,35]. Although many investigations have been carried out on bubble column reactors operating at elevated pressure, to the best of the authors knowledge there is no investigation for bubble column working at sub-atmospheric pressure.

1.4 Objectives and Outline of the Thesis

The main objective of this thesis is to investigate the effect of pressure on the humidification and dehumidification processes in bubble column. A plenty of experimental measurements are performed by utilizing a laboratory test-rig which was designed and built for this objective. Mathematical models are developed to predict the thermal performance which were validated by the experimental results. The present thesis work resulted in two journal papers [31,32]. To achieve the objectives, the scopes of the thesis investigation are given in details:

- Experimental study of bubble column humidifier working under sub-atmospheric pressure and constant inlet water temperature.
- Experimental study on bubble column dehumidifier working at elevated pressures and constant inlet water temperature.
- Experimental study on bubble column dehumidifier working at elevated pressures and constant column liquid temperature.
- Develop ε-*NTU* models to bubble column humidifier and dehumidifier.

- Modify a semi-empirical model of Sherwood number to capture the pressure effects in the dehumidifier.
- Evaluate the effect of column liquid height, superficial velocity and pressure on the thermal performance associated with the total heat transfer rate and effectiveness.

The outline of the thesis is divided into four chapters:

Chapter 1 introduces conventional HDH desalination technologies and the application of bubble columns, emphasizes that the varying pressure operated in the humidification and dehumidification processes is potential and demands to further experimental investigation. The objectives and scopes in this thesis are also specified to answer the stated problems.

Chapter 2 presents experimental and mathematic work on the bubble column dehumidifier in two operating conditions, and details the experimental and numerical results for them. The relationship of effectiveness and *NTU* is applied to the thermal analysis. It further develops a Sherwood number model in consideration of pressure effect.

Chapter 3 describes experimental work on the bubble column humidifier, and presents the simultaneous heat and mass transfer between the air and water streams. An ε-*NTU* model for counter flow heat and mass exchanger is employed. The experimental results of thermal performance are detailed.

Chapter 4 states the conclusion of this thesis and supplies the recommendation for the possible future work.

CHAPTER 2

BUBBLE COLUMN DEHUMIDIFIER

2.1 Mathematical Model

2.1.1 Dehumidifier at Constant T_c

Figure 2-1 shows a schematic of a bubble column dehumidifier where hot-humid air is injected through a perforated plate into a pool of cold fresh water to form a bubbly flow. A coolant is circulated inside a cooling coil immersed in the bubble column to control its temperature and receive the heat released from the hot-humid air. The temperature difference between the air bubbles and the water in the bubble column drives the sensible cooling of the air, while the water vapor concentration (or humidity ratio) difference drives the latent cooling and the condensation occurs at the surface of the bubble (see Figure 2-2a). The turbulent motion of the bubbles ensures a good mixing and a homogeneous temperature in the water column.

The thermal resistance network of the bubble column dehumidifier is shown in Figure 2-2b There are two temperatures namely; the air bubbles temperature (T_a) which decreases from the inlet to the outlet due to the heat and mass transfer, and the temperature of water in the bubble column (T_c) which is fixed by controlling the temperature and flow rate of the coolant in the cooling coil. Giving that $T_a > T_c$, the sensible heat transfer is from the air bubbles to the water in the column, and $\omega_a > \omega_{sc}$, the

latent heat transfer is from the air to the water too. The water vapor carried by the vapor-air mixture diffuses inside the bubble and reaches the bubble-liquid interface where it condenses and joins with the water in the column. The humidity ratio at the air bubble temperature (ω_a) is defined for the gas and vapor mixture inside the bubble while the saturated air humidity ratio (ω_{sc}) is defined at the bubble-liquid interface at the column temperature. At the bubble-liquid interface, it is assumed that the temperature is equal to the column temperature (T_c), thus, the convection resistance from the bubble surface to the liquid in the column is neglected compared with the latent heat transfer.

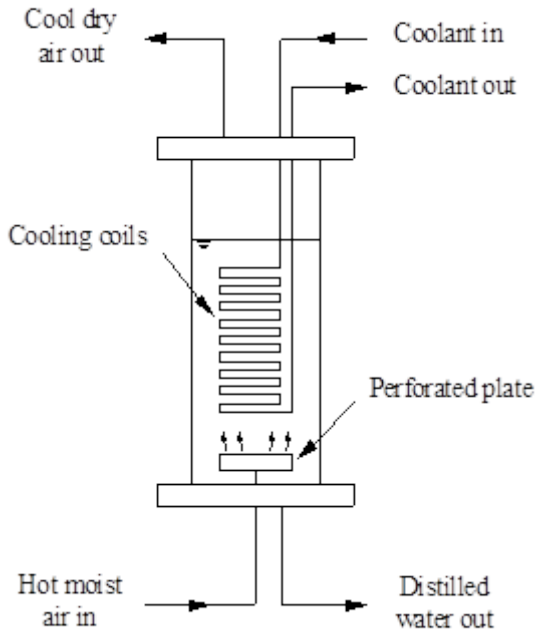

Figure 2-1 Schematic of a bubble column dehumidifier

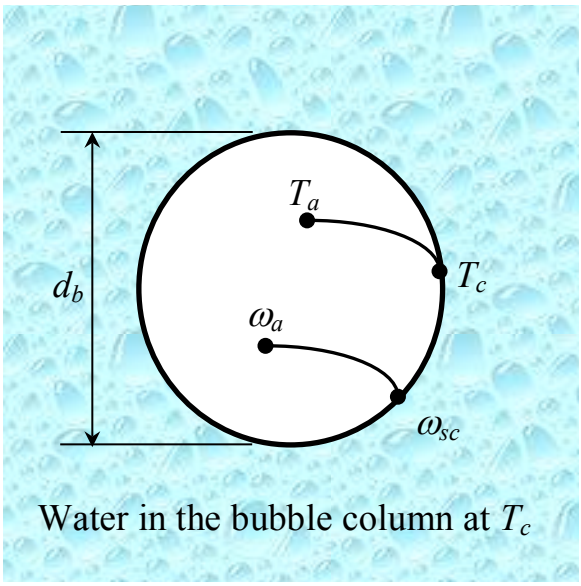

(a)

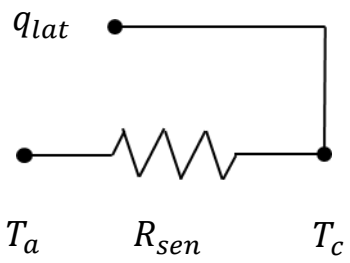

(b)

Figure 2-2 (a) Temperature and humidity ratio gradients inside a bubble; (b) Thermal resistance network

a. Heat and Mass Transfer

Figure 2-3 shows a schematic of the bubble column with a finite volume of cross-sectional area (A_c) and a height (dz) at an elevation (z) from the column bottom. It is assumed that the bubbles are distributed uniformly inside the bubble column and the bubbles diameter has a sauter mean value. The heat loss from the walls of the bubble column as well as the impact heat transfer due to the collision of the bubbles on the cooling coil surface are negligible [11]. The moist air properties are employed with an average air temperature of the inlet and outlet conditions, along with a saturated outlet air assumed.

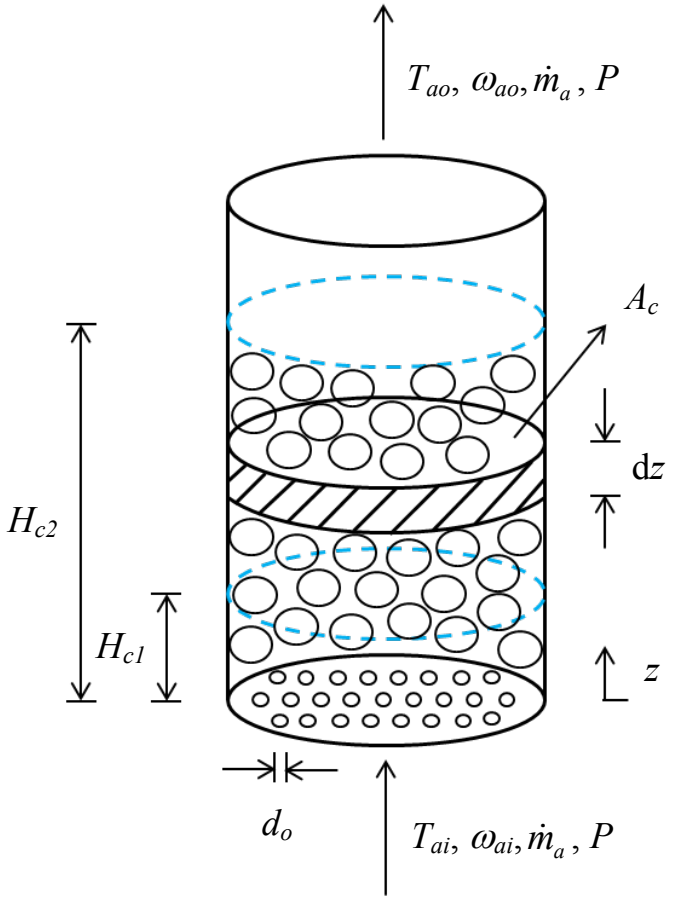

Figure 2-3 Schematic of the bubble column with a finite volume element

The total rate of heat transfer from the air bubbles inside the finite volume to the water in the column is the summation of the sensible and latent heats as given in Equation (2-1).

$$d\dot{q} = d\dot{q}_{sen} + d\dot{q}_{lat} \tag{2-1}$$

The total heat transfer is related to the total enthalpy change of the air as follows,

$$d\dot{q} = -\dot{m}_{da} di_a \tag{2-2}$$

Over a differential height of the liquid in the column (dz), the sensible heat ($d\dot{q}_{sen}$) due to the temperature difference between the air and water, and the latent heat ($d\dot{q}_{lat}$) due to the vapor concentration difference between the air and the saturated air at the bubble-liquid interface (see Figure 2-2a), are given as follows,

$$d\dot{q}_{sen} = ha(T_a - T_c)A_c dz \tag{2-3}$$

$$d\dot{q}_{lat} = h_d a(\omega_a - \omega_{sc}) i_g A_c dz \tag{2-4}$$

where h is the convective heat transfer coefficient between the moist air inside the bubble and the bubble-liquid interface, and h_d is the convective mass transfer coefficient. Combining Equations (2-1) – (2-4) yields,

$$-\dot{m}_{da} di_a = ha(T_a - T_c)A_c dz + h_d a(\omega_a - \omega_{sc}) i_g A_c dz \tag{2-5}$$

where i_g is the specific enthalpy of saturated water vapor, i_a is the enthalpy of air as given by Equation (2-6),

$$i_a = c_{pa} T + i_{fg} \omega \tag{2-6}$$

An important parameter in air–water systems relating the heat and mass transfer coefficients [36] is the Lewis factor Le_f, defined as [37],

$$Le_f = \frac{h}{h_d c_{pa}} \tag{2-7}$$

Substituting Equation (2-7) into Equation (2-5) and rearranging yields,

$$-di_a = \frac{h_d a A_c}{\dot{m}_{da}} \left[Le_f c_{pa}(T_a - T_c) + i_g(\omega_a - \omega_{sc}) \right] dz \tag{2-8}$$

Adding and subtracting the term $Le_f i_{fg}(\omega_a - \omega_{sc})$ into the bracket of Equation (2-8) and using Equation (2-6), yields,

$$-di_a = \frac{h_d a A_c}{\dot{m}_{da}} \left[Le_f(i_a - i_{sc}) - Le_f i_{fg}(\omega_a - \omega_{sc}) + i_g(\omega_a - \omega_{sc}) \right] dz \tag{2-9}$$

For air–water systems, the Lewis factor Le_f approximates to unity [38]. Using $Le_f = 1$ and the thermodynamic relation $i_{fg} = i_g - i_f$ into Equation (2-9) gives,

$$-di_a = \frac{h_d a A_c}{\dot{m}_{da}} \left[(i_a - i_{sc}) + i_f(\omega_a - \omega_{sc}) \right] dz \tag{2-10}$$

Considering $i_f(\omega_a - \omega_{sc})$ is relatively negligible with respect to the air enthalpy difference, Equation (2-10) can be simplified to,

$$-di_a = \frac{h_d a A_c}{\dot{m}_{da}} (i_a - i_{sc}) dz \tag{2-11}$$

Since T_c is constant, it implies that i_{sc} is constant too. In addition, it is assumed that h_d is constant along the bubble column height although it may change due to the local variation of the bubble velocity. However, an effective value of h_d which represents the integrated effect along the column height is considered and will be correlated with the

experimental measurements. Therefore, the variables in Equation (2-11) can be separated and integrated as follows,

$$ln\left(\frac{i_{ai}-i_{sc}}{i_{ao}-i_{sc}}\right)=\frac{h_d a A_c H_{c2}}{\dot{m}_{da}} \tag{2-12}$$

The expression on the left hand side of Equation (2-12) is dimensionless and presents the logarithmic feature of the change of the air enthalpy. The expression on the right hand side of Equation (2-12) is dimensionless too and presents the number of transfer units (*NTU*) in heat and mass exchangers. The *NTU* is defined as follows [39],

$$NTU=\frac{h_d a V_c}{\dot{m}_a} \tag{2-13}$$

where V_c is the volume of the aerated water in the bubble column, which is equal to the product of the cross-sectional area A_c and the aerated water height H_{c2}. Combining Equation (2-12) and Equation (2-13), we obtain the following expression,

$$NTU=ln\left(\frac{i_{ai}-i_{sc}}{i_{ao}-i_{sc}}\right) \tag{2-14}$$

Furthermore, the effectiveness of heat exchanger (ε) is defined as the ratio of actual enthalpy change to maximum enthalpy change at which the exit air temperature approaches the column temperature, hence,

$$\varepsilon=\frac{i_{ai}-i_{ao}}{i_{ai}-i_{sc}} \tag{2-15}$$

Combining Equation (2-14) and Equation (2-15), the relationship between ε and *NTU* is given as,

$$\varepsilon=1-e^{-NTU} \tag{2-16}$$

Equation (2-16) is a well-known relation for a heat exchanger with a phase change (condensation or evaporation) occurs in one of the fluid streams (i.e. one of the fluids is at a constant temperature). Based on the model developed above, the value of the *NTU* can be determined from the experimental measurements of the column liquid temperature and the inlet and outlet air enthalpies. Alternatively, for a given *NTU*, inlet air conditions, and column temperature, we can determine the outlet air temperature and the effectiveness of the bubble column dehumidifier. However, for design purpose, we should know the convective mass transfer coefficient h_d in order to calculate *NTU* for a given bubble column geometry. Therefore, the next section presents a phenomenological model that is adopted from [40] to determine h_d. This model is modified to capture the pressure effect and is calibrated by the experimental results obtained in the present work.

b. The Convective Mass Transfer Coefficient

Mass transfer characteristics in bubble columns has been studied by many investigators [28,41–44]. In these studies, the overall mass transfer from the gas phase (inside the bubble) to the liquid phase (in the column) is governed by the liquid-side mass transfer coefficient and assumed that the gas side resistance is negligible. Different models were proposed to estimate the convective mass transfer coefficient in the liquid phase as a function of the superficial gas velocity, gas holdup, bubble diameter, and gas density. Akita and Yoshida [41] experimentally measured the volumetric mass transfer coefficient in the bubble column and developed a correlation which shows the mass transfer coefficient is proportional to the gas holdup to the power of 1.1. Their empirical correlation was later verified by other experimental evidence [42]. Hikita et al. [44]

proposed a correlation for the volumetric mass transfer coefficient which has an average deviation of 2.5% with the experimental data. Wilkinson and Haringa [28] developed a correlation which estimates the mass transfer coefficient directly from the gas holdup which was measured at different gas densities and pressures. Since the mass transfer coefficient is also depending on the bubble diameter, they scaled the bubble diameter with the density ratio of the gas and liquid phases. Öztürk et al. [43] found that the volumetric mass transfer coefficient is related to the density ratio of the phases based on the measurements of mass transfer coefficient for 50 gas and liquid mixtures at atmospheric pressure. They developed a correlation which predicts the mass transfer coefficient with an average deviation of 13.3% from the experimental measurements.

The above mentioned studies though did not consider the mass transfer coefficient due to the diffusion of vapor through the vapor-gas mixture inside the bubble. When the diffused vapor reaches the bubble-liquid interface, it condenses and joins with the liquid in the column without diffusing into it (because it is the same liquid). On the other hand, the air in the vapor-air mixture is assumed to be undissolvable into the water column since this air is hot, hence; has low solubility. The convective mass transfer coefficient of the gas side was estimated by Narayan et al. [11] by assuming a diffusive boundary layer with a thickness equals the radius of the bubble which is an upper limit for the size of the boundary layer and the associated thermal resistance.

There are several complexities involved in evaluating the mechanism of transport inside the bubble. In the present work, we adopted the model of Miller [40] to determine the convective mass transfer coefficient of the vapor diffuses into vapor-air mixture. The model is modified to capture the pressure effect and is compared with the experimental

data obtained and presented in the next section. The correlation relates Sherwood number to Reynolds number, Schmidt number, and the density ratio of the air and water vapor as given by Equation (2-17),

$$Sh = n_0 Re^{n_1} Sc^{n_2} {\rho_r}^{n_3} \tag{2-17}$$

The Sherwood number, *Sh* is considered as a dimensionless mass transfer coefficient defined as,

$$Sh = \frac{h_d d_b}{\rho_v D} \tag{2-18}$$

where d_b is the bubble diameter which is related to the orifice diameter of the perforated plate, surface tension of water, and the air and water densities as given by Equation (2-19). It is noted that several sample corrections for the bubble diameter were presented in a review article [15]. The following expression cited by Miller [40] and Narayan et al. [11] in a similar system,

$$d_b = \left[\frac{6\sigma d_o}{(\rho_c - \rho_a)g}\right]^{1/3} \tag{2-19}$$

Reynolds number and Schmidt number in Equation (2-17) are given by,

$$Re = \left(\rho_a V_g d_b\right)/\mu_a \tag{2-20}$$

$$Sc = \mu_a/(\rho_a D) \tag{2-21}$$

where V_g is the superficial gas velocity given by,

$$V_g = \frac{\dot{V}_a}{\dot{A}_c} \tag{2-22}$$

The density ratio (ρ_r) in Equation (2-17) is the ratio of the saturated air density to the saturated vapor density at the average air temperature and pressure. The density ratio is introduced to the model suggested by Miller [40] to capture the effect of the pressure on the gas-side mass transfer coefficient. Since, increasing the pressure increases the air density but not the saturated vapor density as it depends only on the temperature. The increase of the air density decreases the bubble diameter which brings the water vapor and air molecules closer to each other. This increases the mass transfer coefficient and consequently the total heat transfer. The introduction of the density ratio was also used by Wilkinson et al. [28] to correct the pressure effect on the heat and mass transfer coefficients in bubble columns. We found that adding the density ratio in the correlation makes it fit well with the experimental data.

The specific area (a) in Equation (2-13) is determined with the following widely-accepted correlation that assumes spherical bubbles [40],

$$a = \frac{6\epsilon}{d_b} \tag{2-23}$$

where ϵ is the gas holdup expressed as follows [45],

$$\epsilon = \frac{V_g}{0.3+2V_g} \tag{2-24}$$

In addition, the gas holdup is related to the initial water height (H_{c1}) and the aerated water height (H_{c2}) in the column as follows [41],

$$\epsilon = \frac{H_{c2}-H_{c1}}{H_{c2}} \tag{2-25}$$

It is important to mention that the overall convective mass transfer coefficient (h_d) in Sherwood number can be calculated experimentally using the number of transfer units (*NTU*) of Equation (2-13). The following Equation (2-26) shows the relationship between *Sh* and *NTU*,

$$NTU = \frac{Sh}{ReSc} \cdot \frac{aH_{c2}}{\rho_r} \tag{2-26}$$

The *ε–NTU* model developed in Equation (2-16) reveals that the bubble column dehumidifier with constant column temperature is similar to a heat exchanger with one fluid at constant temperature (e.g. in evaporation or condensation). The determination of the mass transfer coefficient h_d that appears in the *NTU* equation is calculated from the experimental data and fitted to Equation (2-17). The coefficients in Equation (2-17) will be determined using the experimental data that is discussed in Section 2.3.1. The presented model gives a direct and effective modification to the model suggested by Miller [40] to capture the pressure effect using the density ratio.

The set of equations in the mathematical model are modeled and solved numerically by using Engineering Equation Solver (EES) program [46]. The physical properties of moist air and liquid water are acquired from its built-in functions relying on good accuracy thermodynamic and transport properties database. The non-linear equations are solved iteratively to obtain the outputs of performance evaluations based on the inputs of operating conditions, with graphic solutions generated in plots.

2.1.2 Dehumidifier at Constant T_{wi}

Figure 2-4 shows a schematic of the bubble column dehumidifier. It demonstrates the physical processes that take place in order to help presenting the thermal analysis. In the dehumidification process, hot-humid air is sparged from a perforated plate at the bottom of the bubble column dehumidifier into a pool of cold water to form a bubbly flow. Cold water is circulated inside the cooling coil immersed in the bubble column that receives the heat released from the hot-humid air. The temperature difference between the air bubbles and the water in the bubble column contributes to the sensible cooling of the air. While the water-vapor concentration (or humidity ratio) difference drives the latent cooling and the condensation occurs at the interface of the bubble surface and the water in the column. The inlet temperatures of the air and water are fixed during the dehumidifier test. In this process, the liquid in the column is regarded as a transition phase for the sensible heat transfer, and obtains the vapor condensation from the air moisture stream in form of latent heat transfer. The dissolution of air into the water phase is neglected. The outlet air is assumed in saturated condition due to sufficient contact with water in the column.

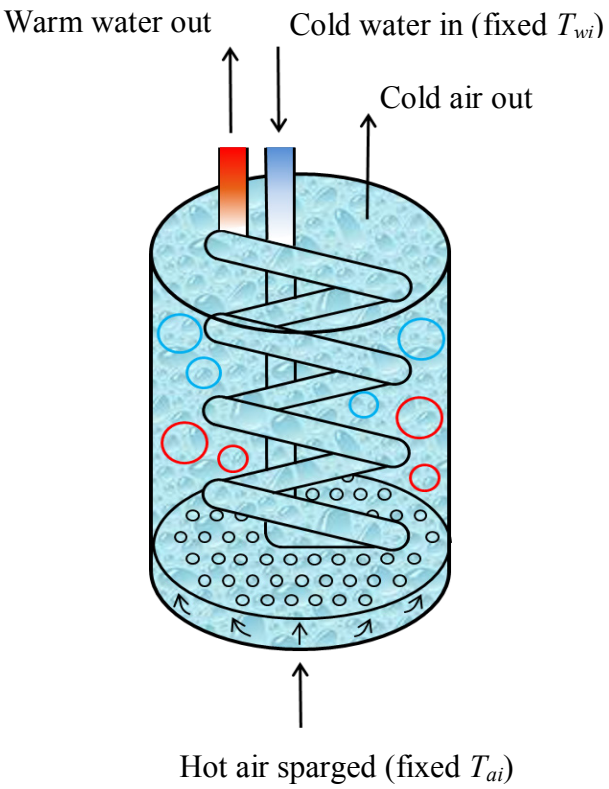

Figure 2-4 Schematic of the bubble column dehumidifier at constant T_{wi}

Figure 2-5 shows a control volume that represents the dehumidification process occurs in the bubble column dehumidifier. The flow configuration of the circulated water inside the coil and the air in the bubble column can be treated as a counter flow heat exchanger. This is similar to the transport processes occur in a cooling tower where heat and mass are transferred between the air and water streams. In the following thermal analysis of the bubble column dehumidifier, the inlet and outlet conditions are measured experimentally and the performance is calculated. The performance is evaluated by calculating the total heat transfer rate and effectiveness (ε). An ε-*NTU* model developed by Braun et al.[39] for counter flow cooling tower is used to determine the effective mass transfer coefficient in the bubble column. The derivation of the model for both cooling tower and bubble column should be the same. The difference between the two models is the surface area available for the simultaneous heat and mass transfer processes. In the cooling tower, this area is the surface area of the packing, however, in the bubble column it is the surface area of the bubbles in the column.

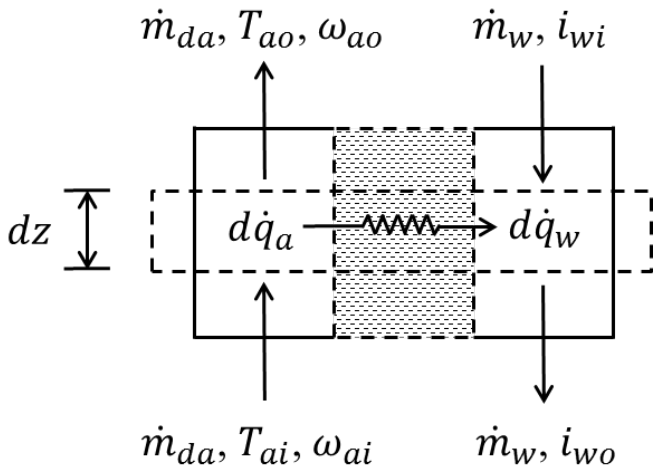

Figure 2-5 A finite volume element in a bubble column dehumidifier with a counter flow configuration

Applying energy balances on the air and water streams of the control volume shown in Figure 2-5 for the dehumidifier,

$$d\dot{q}_a = d\dot{q}_w \tag{2-27}$$

The total heat transfer rate in the air and water sides can be expressed in terms of their total enthalpy changes,

$$d\dot{q}_a = -\dot{m}_{da} di_a \tag{2-28}$$

$$d\dot{q}_w = \dot{m}_w di_w \tag{2-29}$$

Contributing to the majority of the total heat transfer rate in the air stream, the latent heat transfer rate is respected to the increment of humidity ratio, and is given by,

$$d\dot{q}_{lat} = -\dot{m}_{da} i_{fg} d\omega_a \tag{2-30}$$

Analogous to a cooling tower, the mass balance over a finite volume is given by the following differential equation,

$$-d\omega_a = \frac{h_d a A_c}{\dot{m}_{da}} \left(\omega_a - \omega_{sa,w}\right) dz \tag{2-31}$$

where h_d is defined as the convective mass transfer coefficient of the water vapor inside the bubbles. The number of transfer units (*NTU*) for a heat and mass exchanger is given by [39],

$$NTU = \frac{h_d a V_c}{\dot{m}_{da}} \tag{2-32}$$

Integrating Equation (2-31) and using the definition of *NTU* given by Equation (2-32), the following expression is obtained to calculate *NTU*.

$$NTU = \int_{\omega_{a,i}}^{\omega_{a,o}} \frac{d\omega_a}{(\omega_{sa,w-}\omega_a)} \tag{2-33}$$

The integration of Equation (2-33) is made by assuming a linear relationship between the humidity ratio of the saturated air and the water temperature since the variation in the water temperature is very small along the bubble column. The effectiveness is defined as the ratio of the actual total heat transfer rate to its maximum approaching value of the stream having minimum heat capacity. In the present work, the air stream has the minimum heat capacity and therefore an expression for its effectiveness is given by,

$$\varepsilon = \frac{i_{ao}-i_{ai}}{i_{sa,wi}-i_{ai}} \tag{2-34}$$

where $i_{sa,wi}$ is the enthalpy of saturated air at entering water temperature, which is the maximum possible temperature for the exit air in a counter flow heat exchanger.

The heat capacity ratio (*HCR*) for a heat and mass exchanger was defined by Narayan et al. [3,26] as the ratio of maximum possible total enthalpy change between the cold stream and hot stream (*HCR* < 1),

$$HCR = min\langle \frac{i_{sa,wi}-i_{ai}}{i_{wi}-i_{w,ai}}, \frac{i_{wi}-i_{w,ai}}{i_{sa,wi}-i_{ai}} \rangle \tag{2-35}$$

Analogous to a counter flow heat exchanger, the relationship of the effectiveness and *NTU* is given by Equation (2-36) [39],

$$\varepsilon = \frac{1-exp[-(1-HCR)\cdot NTU]}{1-HCR\cdot exp[-(1-HCR)\cdot NTU]} \tag{2-36}$$

In order to determine the mass transfer coefficient from Equation (2-32), the specific area (a) in the bubble column is required. The specific area is given by Equation (2-37) assuming that the bubbles are of mean sauter diameter [40],

$$a = \frac{6\epsilon}{d_b} \tag{2-37}$$

The gas holdup in Equation (2-37) is given by the following expression provided by Joshi and Sharma [45],

$$\epsilon = \frac{V_g}{0.3+2V_g} \tag{2-38}$$

where V_g is the superficial velocity calculated by dividing the actual air flow rate by the cross sectional area of the bubble column. The gas holdup (ϵ) can be also expressed by the following relationship which relates the aerated liquid height in the bubble column (H_{c2}), to the static liquid height (H_{c1}), provided by Akita and Yoshida [41],

$$\epsilon = \frac{H_{c2}-H_{c1}}{H_{c2}} \tag{2-39}$$

The aerated liquid height (H_{c2}) is used to determine the aerated volume (V_c) which appears in Equation (2-32) by multiplying it by the cross-sectional area (A_c).

Finally, the following expression given by Miller [40] and Narayan et al. [11] in a similar system is used to determine the bubble mean diameter.

$$d_b = \left[\frac{6\sigma d_o}{(\rho_w-\rho_a)g}\right]^{1/3} \tag{2-40}$$

2.2 Experimental Work

2.2.1 Dehumidifier at Constant T_c

A laboratory scale test-rig was designed and constructed to study the heat and mass transfer processes between moist air and liquid in a bubble column dehumidifier working under atmospheric and elevated pressures. A photograph of the bubble column dehumidifier during the experimental test is shown in Figure 2-6.

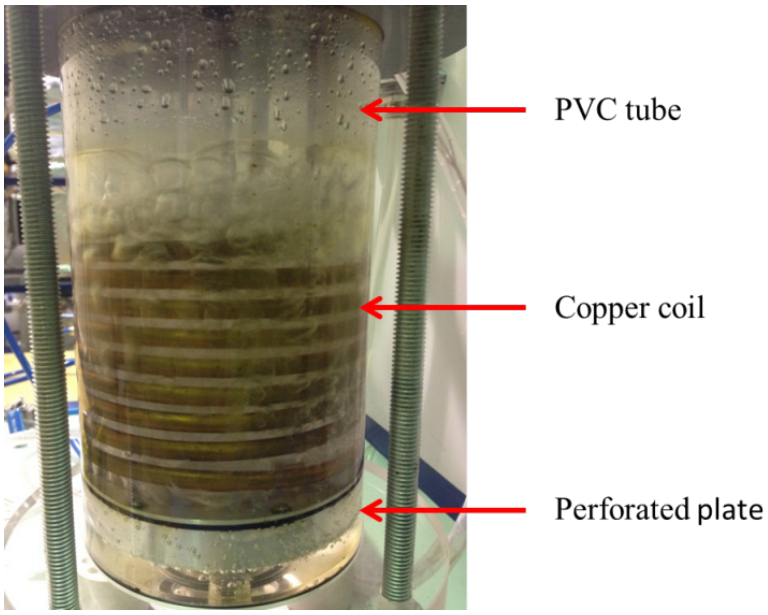

Figure 2-6 Photo of the bubble column dehumidifier

Figure 2-7 shows a schematic diagram of the test-rig used in this study. The apparatus consists of a compressor (1), bubble column humidifier (3), bubble column dehumidifier (9), flow control valves (15, 17), pressure control valves (2, 10), make-up tank (16), and a constant temperature bath (20).

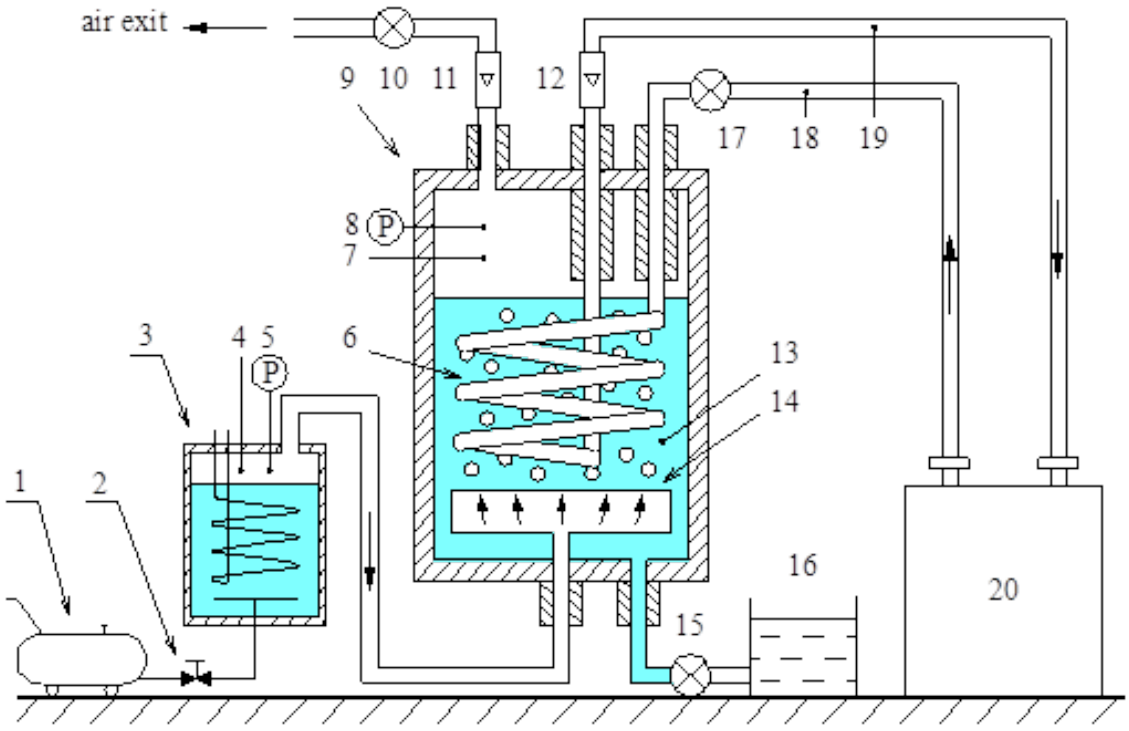

Figure 2-7 Schematic of the laboratory scale test-rig for dehumidifier test at fixed T_c

(1) Air compressor, (2, 10) pressure control valves, (3) bubble column humidifier (4, 7, 13, 18, 19) thermocouples, (5, 8) absolute pressure sensors, (6) cooling coil, (9) bubble column dehumidifier, (11, 12) rotameters, (14) perforated plate, (16) make-up tank, (15, 17) flow control valves, and (20) constant temperature bath

Air is supplied from the compressor (1) to be heated and humidified in the bubble column humidifier (3), and then it flows to the dehumidifier (9) where it is cooled and dehumidified. For the water loop, hot water in the humidifier coil is circulated between the coil and a constant temperature bath (not shown in the schematic), and cold water in the dehumidifier coil is circulated between the cooling coil (6) and the constant temperature bath (20). The bodies of the bubble column humidifier and dehumidifier are made from transparent PVC tubes of 10 mm thickness, 100 mm inside diameter, and 250 mm height (with a tolerance of ±0.1 mm). The heating and cooling coils are made of seamless copper tubes of 9.5 mm outside diameter, 0.9 mm thickness, and spiraled inside the bubble column to 90 mm vertical height. This height does not include the two vertical pipes that connect the coil to the outside tubing. These two pipes are insulated with 3 mm thickness insulation tape as shown in Figure 2-7 to reduce the convection heat transfer with air. The cooling and heating coils in the dehumidifier and humidifier respectively are connected to constant temperature baths with an adjustable range of 0 – 80 °C. An air sparger (14) made of stainless steel cylindrical box of 98 mm outside diameter and 18 mm height is located on the bottom of the bubble column where air is injected into the water. The top cover of this box is a perforated plate with 83 holes of 1 mm diameter drilled on its surface with staggered distribution of 9 mm pitch. The two bubble columns are supplied with small tanks (16) to charge, empty, and adjust the water level inside the columns.

The thermocouples used in the apparatus (4, 7, 13, 18, 19) are K-type thermocouples of 1.5 mm sheathed probe diameter which are connected to Fluke 2680A high precision analog input module and data logger. This module is equipped with a Platinum RTD

cold-junction compensation unit of ±0.1 K accuracy. The thermocouples and the data logging system has an estimated combined uncertainty of ±0.25 K. Thermocouple (4) measures the outlet temperature of air in the humidifier, and thermocouple (7) measures the outlet temperature of air in the dehumidifier. A rotameter (11) is installed to measure the flow rate of air with a range of 0.5 – 4.5 ft^3/min and an uncertainty of ±2.5%. The flow rate and the pressure of the air are adjusted by valves (2, 10). Another rotameter (12) is installed to measure the flow rate of the coolant in the cooling coil with a range of 0.8 – 8 l/min. The flow rate of the cooling water is adjusted by valve (17). Absolute pressure sensors (5, 8) are installed at the top of each bubble column with a digital readout of a range 0 – 100 psia (0 – 689.5 kPa) and an uncertainty of ±0.1 psia (±0.7 kPa) to measure and record the absolute pressure of the air inside the columns. The water level in the column is directly observed and measured through the transparent tubes. The average aerated water height (H_{c2}) is measured and verified with the calculated value from the gas holdup Equation (2-39) and the initial water height (H_{c1}). The experimental tests were conducted using distilled water inside the bubble columns and the cooling and heating coils. The two bubble columns (the humidifier and the dehumidifier) and all connections are insulated with 25 mm glass wool insulations during the operation, thus the overall heat loss can be neglected.

a. Experimental procedure

The following is the experimental procedure followed before and during the recording of each experimental run. The air pressure inside the column is controlled by valves (2) and (10) to the desired value. The experiments were conducted at four operating absolute

pressures; 15 psia (103.4 kPa), 20 psia (137.9 kPa), 25 psia (172.4 kPa), and 30 psia (206.8 kPa). At each pressure, the air flow rate was changed to cover a range of superficial velocity of 2 – 18 cm/s. During a certain superficial velocity, the temperature of water in the column is fixed by adjusting the flow rate and temperature of the coolant. The water level in the bubble column is adjusted to initial heights of 3, 5, and 7 cm from the perforated plate before air flows using the make-up tank (16). Although the cooling coil height is 9 cm, the aerated bubble column height during the experimental measurements was more than 9 cm except for the 3 cm case where there was a portion of the coil uncovered. We repeated the experimental reading for the 3 cm case after covering that portion of the coil and we didn't notice a significant difference in the exit air temperature. This ensures that the convection heat transfer from the air to the coil surface after it leaves the bubble column is negligible with respect to that one in the bubble column. All temperatures and pressures are recorded automatically by digital data loggers every 5 seconds until a steady state condition is approached (at which the variables are changing only within their uncertainty band).

b. Instrument calibration and uncertainty analysis

To improve the precision of the measurements, a careful calibration of all instruments was performed and the measured data was compared with standard values. The thermocouples were calibrated with a liquid-in-glass thermometer which has a 0.1 K least count while the pressure transducers were calibrated using a dead weight tester to ensure that their readings are accurate to the standard values provided by the manufacturers.

The flow rate measured by the rotameter is corrected due to the difference in the moist air density from the dry air at the STP condition (Standard Temperature and Pressure) for which it was calibrated by the manufacturer. Since the air flow in the rotameter is mainly inviscid, the flow rate is proportional to the square root of the air density. Therefore, a correction to the air flow rate is given by Equation (2-41) below. On the other hand, the rotameter was installed at the humidifier exit where cold air flows through to reduce the effect of condensation.

$$\frac{\dot{V}_{a,m}}{\dot{V}_a} = \sqrt{\frac{\rho_{a,STP}}{\rho_{ai}}} \tag{2-41}$$

The uncertainty mainly arises from the instruments, experiment condition, and observations of measured quantities. Uncertainty analysis is essential to evaluate the accuracy of each calculated result. In this work, the uncertainty of the calculated results is determined using the method described by Coleman and Steele [47]. Based on the uncertainty of each instrument previously stated in previous paragraphs, the uncertainty of each calculated parameter is determined using the uncertainty propagation function in EES commercial software [46]. The uncertainty bars are shown in the results figures that are presented in "Results and Discussion" section.

2.2.2 Dehumidifier at Constant T_{wi}

A schematic of the experimental setup (see Figure 2-8) provides the main components and the basic flow paths in the dehumidifier test. Figure 2-9 shows a photograph of the laboratory scale test-rig without compressor.

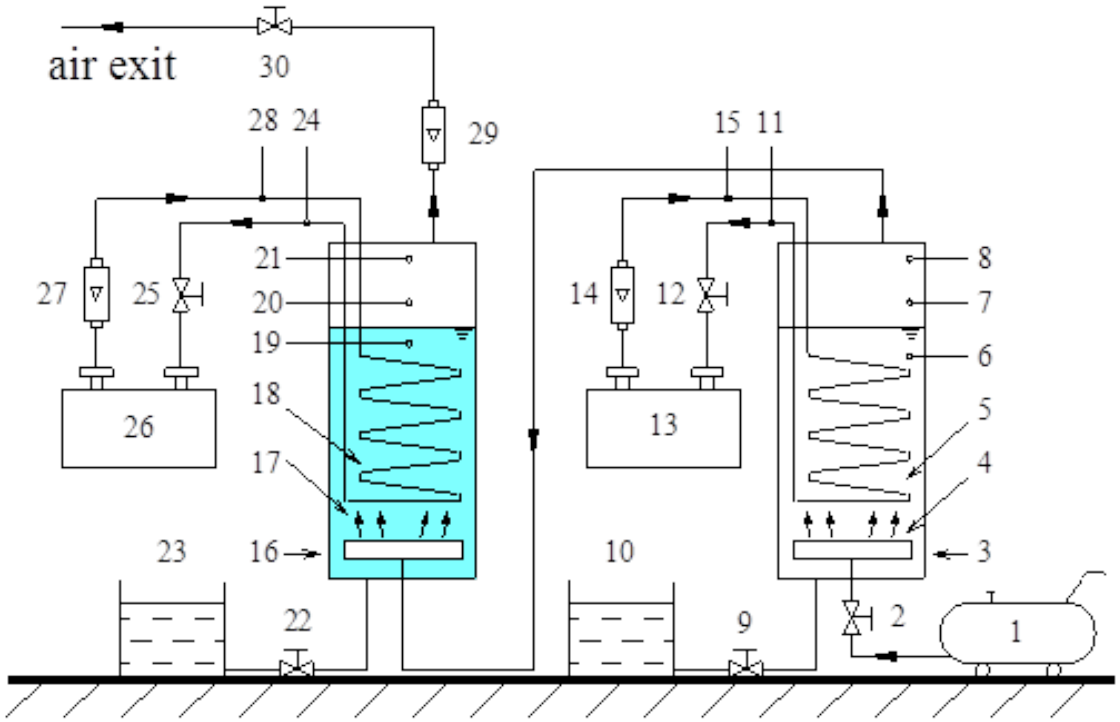

Figure 2-8 Schematic of the experimental setup for dehumidifier test at fixed T_{wi}
(1) air compressor, (2, 9, 12, 22, 25, 30) valve, (3) bubble column humidifier, (4, 17) perforated plates, (5, 18) copper coils, (6, 7, 11, 15, 19, 20, 24, 28) thermocouples, (8, 21) absolute pressure sensors, (10, 23) make-up tanks, (13) water heater, (14, 27, 29) rotameter, (16) bubble column dehumidifier, (26) water chiller

Figure 2-9 Photo of the laboratory scale test-rig without showing the compressor and vacuum pump

For the bubble column dehumidifier tests at elevated pressures, a compressor (1) compresses the air into the bubble column humidifier first then the air flows through the dehumidifier while the vacuum pump is not connected. The pressure and flow rates are controlled by a set of valves (2, 9, 12, 22, 25, and 30). The bubble columns are filled with water to a certain level and the temperature of the water in the columns is controlled by heating and cooling coils inserted inside the humidifier and dehumidifier respectively. Both bubble columns have perforated plates (4, 17) at its bottom where air is sparged through its holes and bubbles aerate the columns.

The structure and geometry of both bubble columns are the same. The external body of the bubble columns is made of transparent PVC tubes of 100 mm inside diameter, 10 mm thickness, and 250 mm height. The tubes are enclosed by two cover plates at the top and bottom where the air inlet and exit ports as well as the measuring instruments are connected. The external surface of the columns was insulated by glass wool blanket of 5 cm thickness to reduce the heat loss or gain to or from the surroundings. A copper coil is installed inside each bubble column to provide the heating or cooling load needed during the experiments. The copper coils have an outside diameter of 9.5 mm, a wall thickness of 0.9 mm, and is spiraled to a helical height of 90 mm with a turn outside diameter of 98 mm. Hot and cold waters are circulated inside the coil in the humidifier and dehumidifier respectively. A water chiller (26) (Thermal Scientific model Accel 500 LC) is connected to the cooling coil installed inside the dehumidifier which provide a cooling capacity up to 500 W and a temperature range of 0 – 80 °C. The heating coil in the humidifier is connected to a constant temperature circulating bath (13) (Omega model HCTB-3010)

which provides a heating capacity up to 1000 W and an adjustable temperature range of 20 – 95 °C.

The air is sparged through the perforated plates (4, 17) installed at the bottom of each bubble column which distribute the air and generate bubbles. The perforated plate consists of a stainless steel cylindrical box of 98 mm outside diameter and 18 mm height. A plate covers this box and has 83 holes of 1 mm diameter each drilled in a staggered distribution with a pitch of 9 mm. The air enters at the bottom of the perforated plate box through stainless steel tube and hose. During the experimental tests, the perforated plate and fittings causes a maximum pressure drop of a 0.12 bar (1.7 psia) at the highest flow rate tested. The level of water in the bubble column is adjusted using make-up tanks (10, 23) which are connected to the bottom of each bubble column.

The operating parameters of flow rate, temperature, and pressure are measured using rotameters (14, 27, 29), thermocouples (6, 7, 11, 15, 19, 20, 24, 28) and absolute pressure gauges (8, 21) respectively. The air flow rate is measured using the rotameter (29) which has a range of 0.5 – 4.5 ft^3/min (236 – 2124 cm^3/s) and an uncertainty of ±2.5%. The water flow rates in the heating and cooling coils are measured using rotameters (14, 27) which have a range of 0.8 – 8 L/min. All thermocouples are of K-type connected to a 12-channel temperature logger (Omega, RDXL 12SD). The thermocouples and the data logger system have a combined uncertainty of ±0.25 K. The absolute pressure of the air inside the bubble columns is measured by digital pressure gauges (Omega, DPG1000B-100A) which have a range of 0 – 100 psia (0 – 6.89 bar absolute) and an uncertainty of ±0.1 psia ($\pm 6.89 \times 10^{-3}$ bar). The water level in the columns is measured directly by a ruler attached to the outside surface of the bubble columns. The hydrostatic pressure of the

liquid in column and the pressure drop in the perforated plate are considered in the measured pressure during the dehumidifier test. The absolute pressure of moist air in the rotameter which determines its density is obtained from the pressure measurements of humidifier (8) and dehumidifier (21) along with total pressure drop mentioned above.

a. Experimental procedure

Before the experimental test starts, gas leakage test is performed to avoid any air leakage from the system. The temperatures from all thermocouples are checked before the implementation of any heating or cooling loads to guarantee a uniform temperature environment. Every run is accomplished to when a steady state condition is achieved at which all measuring variables fluctuate within their uncertainty tolerances, and continuously carried out for new experimental set conditions.

Water level in the bubble column dehumidifier was adjusted to the desired level (3, 5, or 7 cm) using the make-up tank (23). Similarly, the water level in the humidifier was fixed at 5 cm using the make-up tank (10). In the dehumidifier test, the inlet air temperature to the bubble column dehumidifier was fixed at 45°C by adjusting the water column temperature in the humidifier. The inlet water temperature to the cooling coil in the dehumidifier was fixed at 10 °C by setting the temperature of the water chiller (26). The pressure of the dehumidifier was controlled by the valve (30) located at the exit air pipe of the dehumidifier. The elevated pressures tested in the bubble column dehumidifier were set at 20 psia (1.38 bar), 25 psia (1.72 bar), and 30 psia (2.07 bar). The air flow rate through the dehumidifier was adjusted by the valve (2) and was read by the rotameter

(29). The range of the air flow rate tested was 0.5 – 2.25 ft^3/min (236 – 1062 cm^3/s) corresponding to superficial velocity of 3 – 20 cm/s.

b. Instrument calibration and uncertainty analysis

The air flow rate measured by the rotameter (29) is corrected considering that the actual density of the moist air during the experiment is different from the dry air density at standard temperature and pressure (STP) condition at which the rotameter scale was calibrated by the manufacturer. The relationship of the flow rate and density in calibration has been mentioned in the foregoing Section 2.2.1.

Uncertainty analysis is performed to all experimental data to confirm that the measurement accuracy is consistent with the predicated results. This analysis was conducted using Engineering Equation Solver software (EES) [46] knowing the absolute or relative uncertainty of each physical parameter.

2.3 Results and Discussion

2.3.1 Dehumidifier at Constant T_c

The variation of the air exit temperature from the dehumidifier with the superficial velocity and pressure is shown in Figure 2-10. The inlet air temperature is fixed at 45 °C, the temperature of water in the column is fixed at 15 °C, and the initial water height is 5 cm. It is noticed that the air exit temperature decreases with the increase of the superficial

velocity while it increases slightly with the pressure. It is known that the mass transfer coefficient increases with the increasing superficial gas velocity due to the increase of the turbulent dissipation rate in the column [24,34,35]. The increase of the mass transfer coefficient leads to the increasing total heat transfer rate which accounts for the progressive decrease of the air exit temperature. On the other hand, the pressure increases the air mass flow rate for a given superficial velocity due to the increase of the air density. Consequently, it increases the amount of sensible heat transfer from the air stream as it approaches the column temperature. Therefore, the enthalpy difference between the inlet and exit air decreases which leads to the slight increase of the air exit temperature with the pressure.

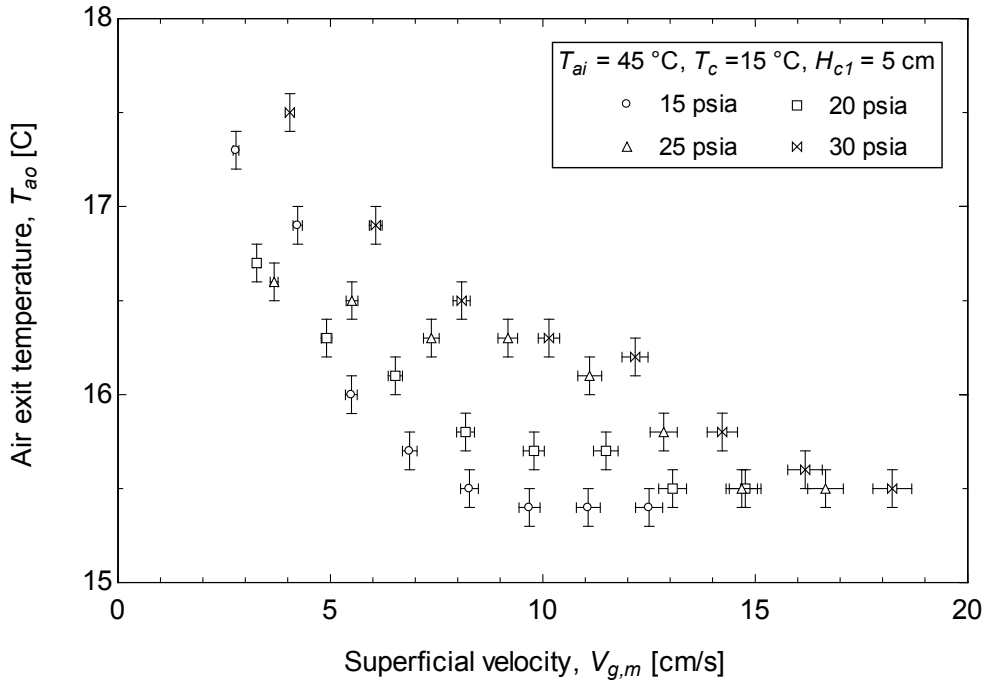

Figure 2-10 Air exit temperature from the dehumidifier at different pressures and superficial velocities

Figure 2-11 shows that the heat transfer rate is nearly independent on the water height at all measured superficial velocities. This finding agrees well with the previous research [11–13]. However, Figure 2-12 shows a slight increase in the effectiveness with the initial water height. This variation is very small and within the uncertainty of the measured temperatures. Therefore, in the following discussion, we will present only data at 5 cm initial water height. Although the effectiveness model showed that the *NTU* is proportional to the column height, it also depends on the specific area which is a function of the gas holdup. It was reported by many researchers that the gas holdup is affected by the column height at aspect ratio (height-to-diameter) less than 5. In our experiment, this ratio is about 1. This indicates that the gas holdup decreases with the column height due to the wall effect and consequently it decreases the specific area. The decrease of the specific area repeals the effect of the column height. This finding suggests that the effect of column height at lower bubble column aspect ratio needs further investigation.

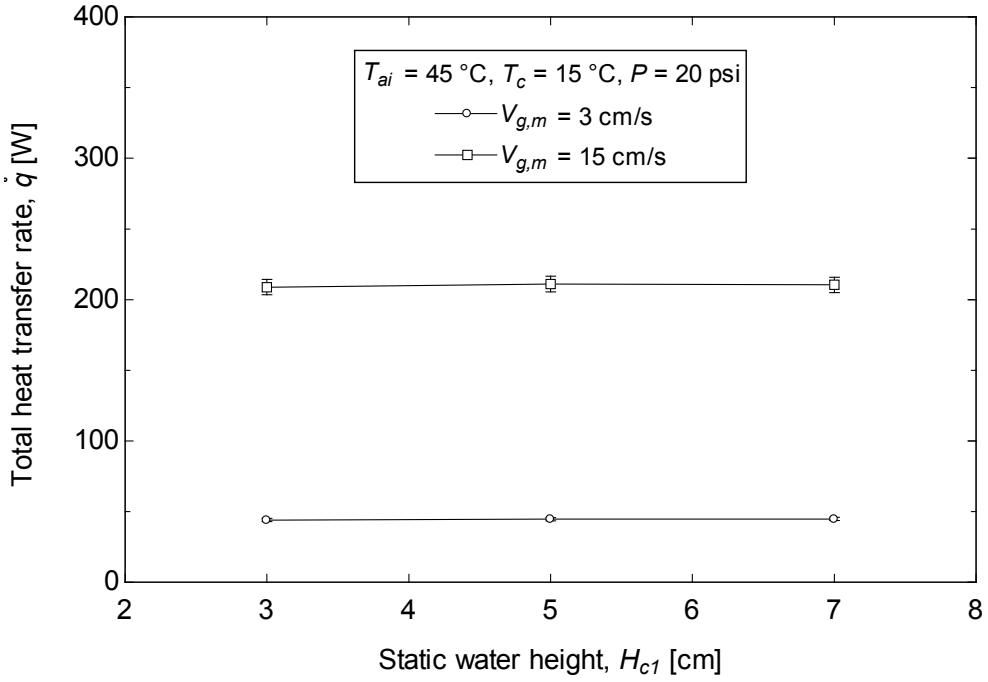

Figure 2-11 Effect of the bubble column initial water height on the total heat transfer rate

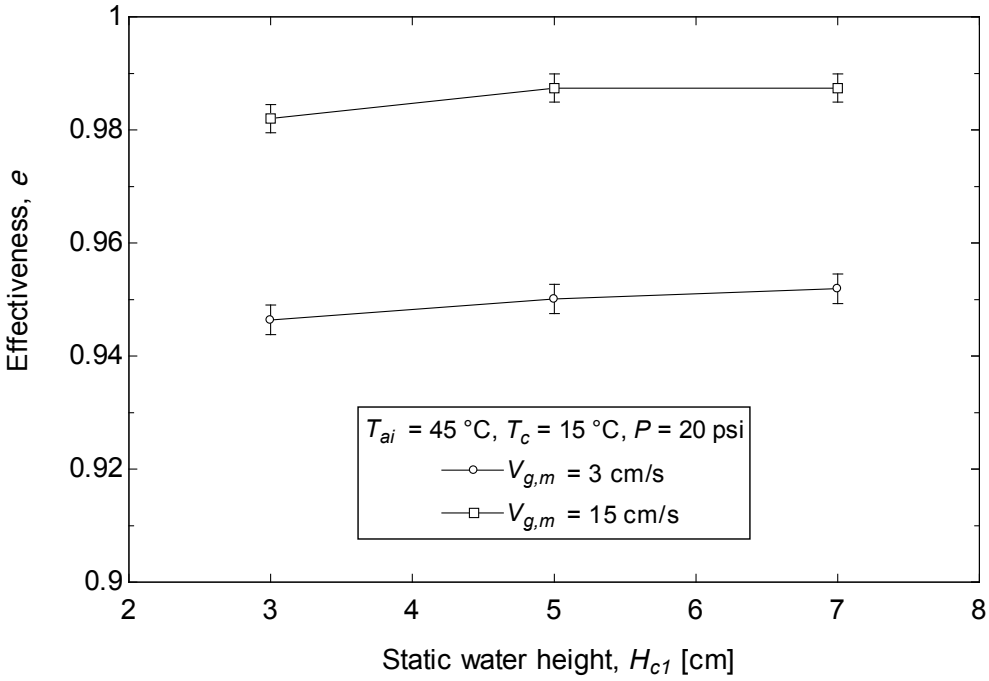

Figure 2-12 Effect of bubble column initial water height on the effectiveness

Figure 2-13 presents the experimental measurements of Sherwood number as calculated from Equation (2-18) varies with the dimensionless groups $Re^{0.43}Sc^{0.21}\rho_r^{1.3}$. The figure shows a straight line with a slope approximates to 0.32, treated as the coefficient on the right hand of Equation (2-17) (i.e. n_0). The coefficients $n_0 - n_3$ in Equation (2-17) are determined using a regression method to best fit the experimental data. The regression method revealed values of $n_1 = 0.43$, $n_2 = 0.21$, and $n_3 = 1.3$. It is important to mention that these coefficients are similar to what have been obtained by the referred publications [40,48] except for the exponent of the density ratio (n_3) and the slope (n_0). The density ratio introduced to the model captures the overall effect of the pressure in the bubble column dehumidifier. The predicated Sherwood number calculated using Equation (2-18) has an average deviation of 5% from the experimentally measured ones.

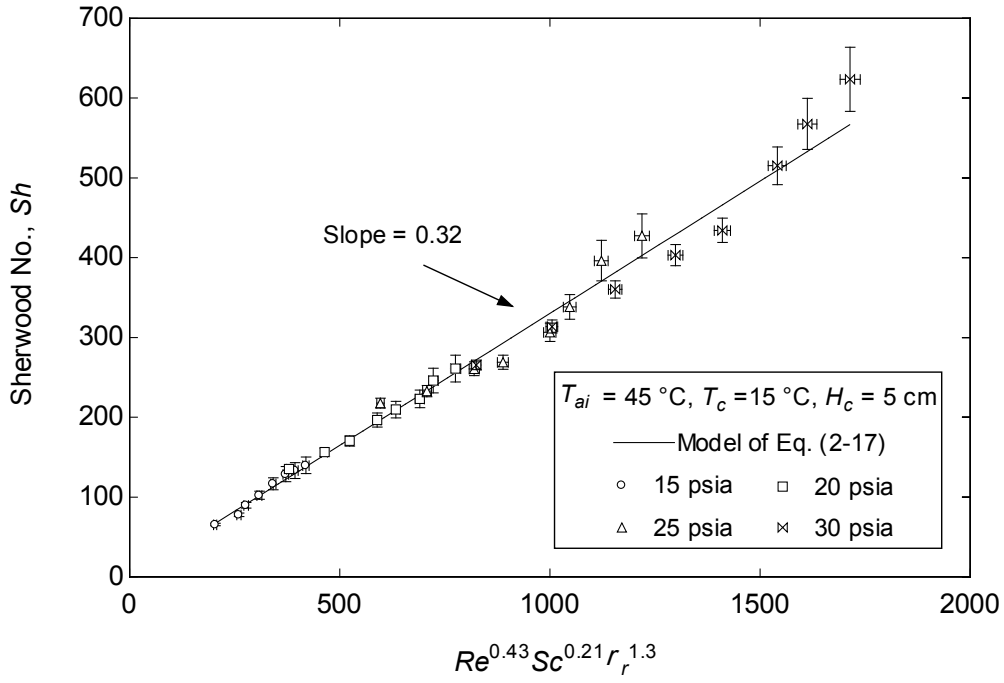

Figure 2-13 Empirical correlation of Sherwood number with other dimensionless groups

Figure 2-14 shows the variation of the total heat transfer rate with the superficial velocity at different pressures. The total heat transfer rate is linearly proportional to the superficial velocity and it is observed that there is a slight increase with the pressure. The increase of the superficial velocity increases the gas holdup (as given by Equation 2-24) which consequently increases the specific area and the total heat transfer rate. On the other hand, the increase of the pressure decreases the bubbles size and increases the gas holdup which again increases the specific area and the total heat transfer rate. Similar effect of the pressure on the bubble size and gas holdup was also observed by [28,34,35]. Some researchers [11,12,15,28,42] explained the increase of the heat transfer with the superficial velocity by the increase of the turbulent dissipation rate in the bubble column. Figure 2-14 also shows the model prediction of the total heat transfer rate as indicated by the straight lines. It is clearly shown that there is a good agreement between the model and the experimental data.

Figure 2-15 shows the variation of the effectiveness with the superficial velocity at different pressures. The curves demonstrate that the effectiveness decreases slightly with the pressure while it increases appreciably with the superficial velocity. Based on the $\varepsilon - NTU$ model developed in the present work and the definition of the *NTU* given by Equation (2-13), the increase of the superficial velocity leads to an increase in the specific surface area and the mass transfer coefficient which consequently increases the *NTU*. This explains the increase in the effectiveness with the superficial velocity which could be also noticed by the decrease of the exit air temperature (see Figure 2-10). On the other hand, the increase of the pressure increases the air density which in turns decreases the *NTU*. A comparison between the heat transfer rates calculated by the model of

Equation (2-17) and the measured ones are presented in Figure 2-16. It is demonstrated that there is an excellent agreement between the model prediction and the experimental results.

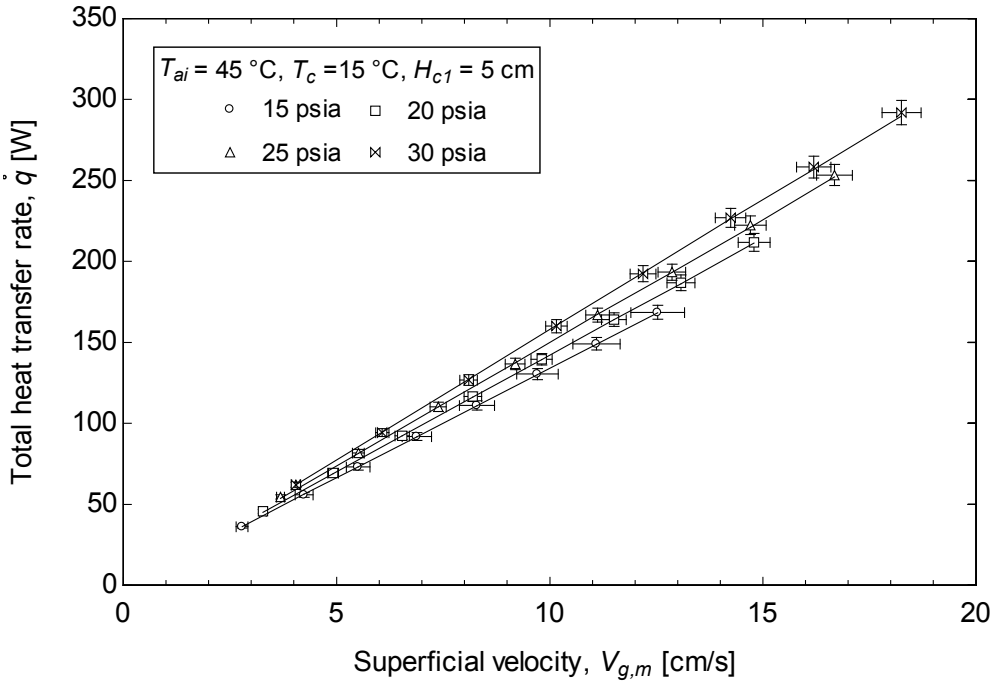

Figure 2-14 Effect of the superficial velocity and the pressure on the total heat transfer rate, the lines indicate the model predictions

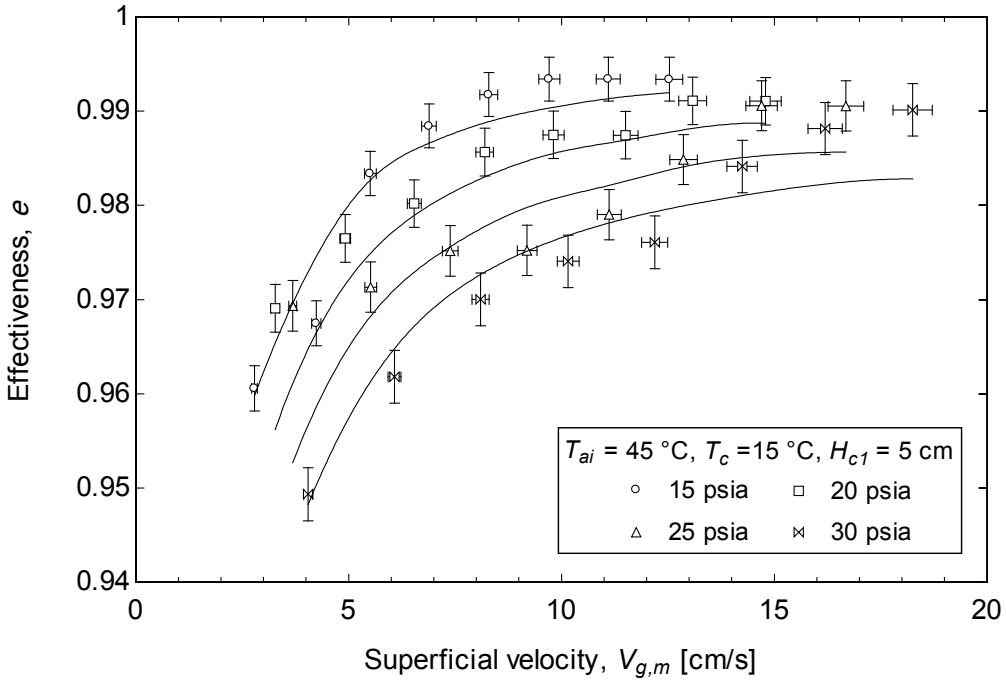

Figure 2-15 Effect of the superficial velocity and the pressure on the effectiveness, the lines indicate the model predictions

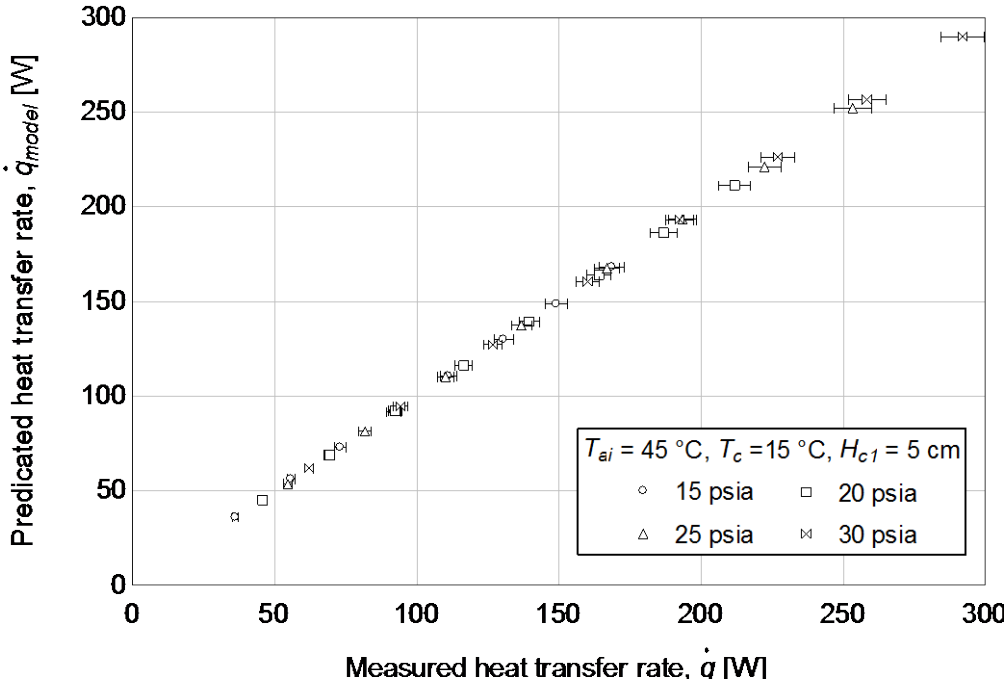

Figure 2-16 A comparison between the predicated and the measured heat transfer rates

Figure 2-17 shows the effectiveness of the bubble column dehumidifier calculated from Equation (2-15) for the measured data as it changes with the *NTU* calculated from Equation (2-13) using the correlation of the mass transfer coefficient by Equation (2-17). It is shown that the effectiveness increases with the increase of the *NTU* at all operating conditions. In addition, it is verified that the experimental results agree well with the developed ε-*NTU* model presented by Equation (2-16). Specifically, the bubble column in this investigation can be treated as a heat exchanger with one fluid at constant temperature such as a boiler or condenser. Interestingly, the effectiveness of the bubble column approaches unity at high values of *NTU*.

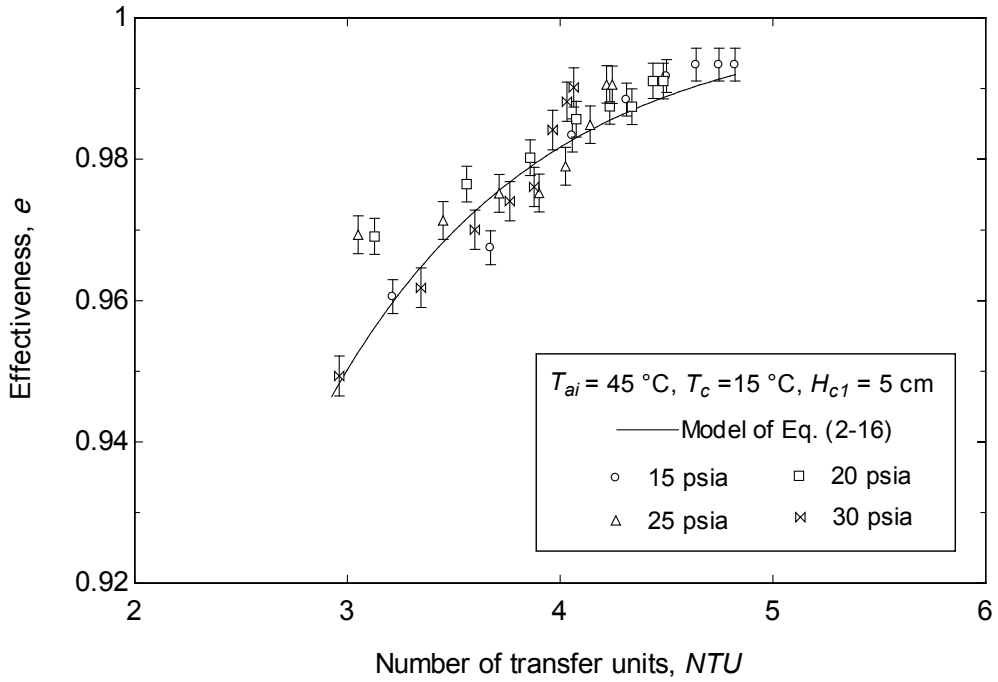

Figure 2-17 Effectiveness vs. *NTU* at various pressures and superficial velocities

2.3.2 Dehumidifier at Constant T_{wi}

Experimental measurements are conducted for the bubble column dehumidifier under different operating conditions. The parameters that are varied in the experimental runs are the static liquid height, superficial velocity, and pressure. However, the inlet temperatures of both air and water are fixed for the bubble column dehumidifier. The thermal performance of the bubble column is presented by calculating the total heat transfer rate and the effectiveness. In addition, the mass transfer coefficient is illustrated under varying superficial velocity and pressure.

Figure 2-18 shows the outlet temperatures of air and water in the dehumidifier at elevated pressures and different superficial velocities. As shown in the figure, the outlet air temperature decreases with the superficial velocity while the outlet water temperature increases. The decrease of the exit air temperature could be attributed to the increase of the heat transfer coefficient with increasing the superficial velocity due to the enhanced turbulence [15]. On the other hand, the increase of the air flow rate directly increases the sensible heat transfer rate which is collected by the circulating cooling water in the coil and leads to an increase of the exit water temperature.

The effect of pressure on the outlet air and water temperatures in the dehumidifier is also shown in Figure 2-18. In the dehumidifier, the exit air temperature increases at higher pressures which could be explained by the increase occurs in the mass transfer coefficient with the pressure as will be shown in Figure 2-21. In addition, the exit water temperature in the dehumidifier is decreased at an elevated pressure. This is perhaps due to the decrease of the total heat transfer rate as a result of the increasing exit air temperature provided with a constant air mass flow rate.

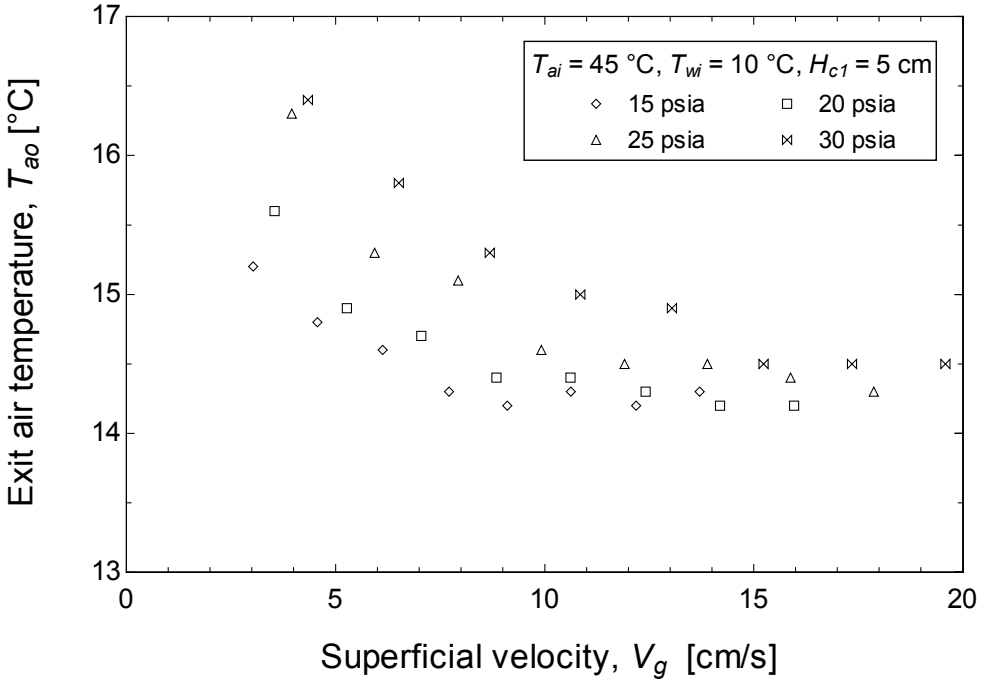

(a)

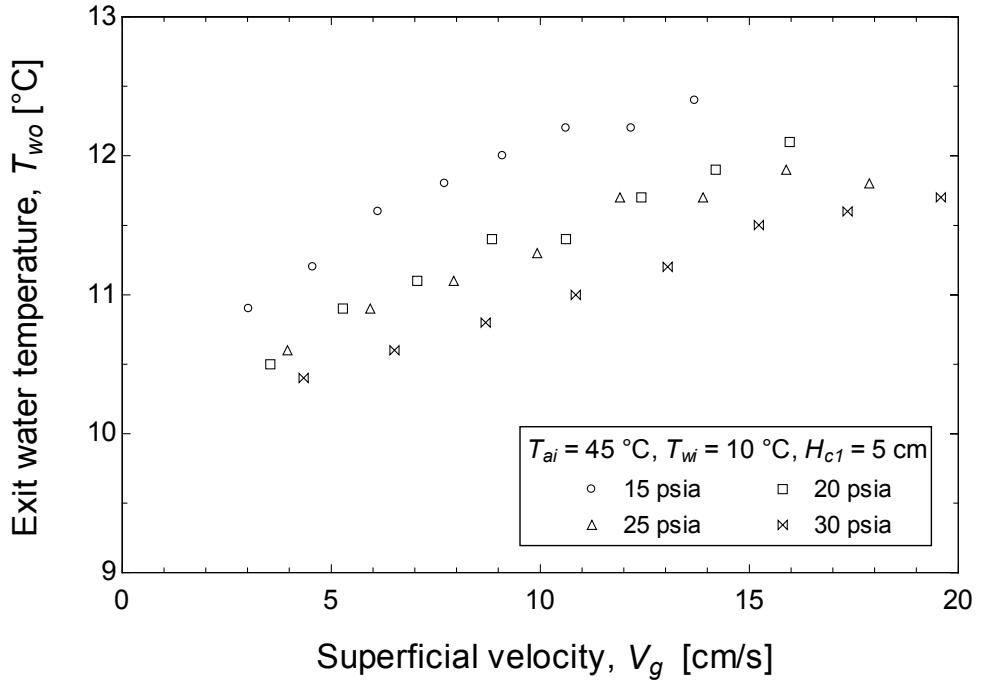

(b)

Figure 2-18 Outlet temperatures of air (a) and water (b) in the bubble column dehumidifier at different pressures and superficial velocities

The column liquid height discussed herein is the static height of the water in the column. During the experimental runs, the static height was varied in the range of 3 – 7 cm which does not immerse the coil totally. However, the aerated liquid height after bubbling effectively covered the coil. It was not possible to increase the static liquid height more than 7 cm as there is no much space and the water in the column will flow with the air stream. The influences of varying the column liquid height on the total heat transfer rate and effectiveness for dehumidifier case were determined. As shown in Figure 2-19, the effect of column liquid height in the dehumidifier is found insignificant to either the total heat transfer rate or the effectiveness which agrees well with these previous studies [11,12,31]. Accordingly, the remaining experimental results exclude the liquid height effect and will show all dehumidifier tests at a liquid height of 5 cm.

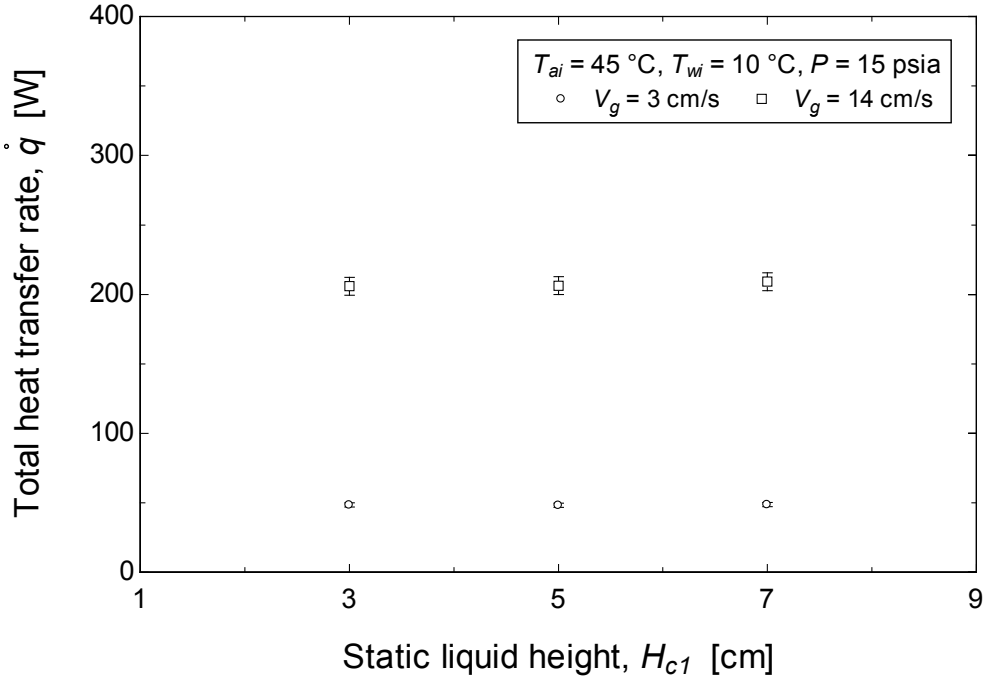

(a)

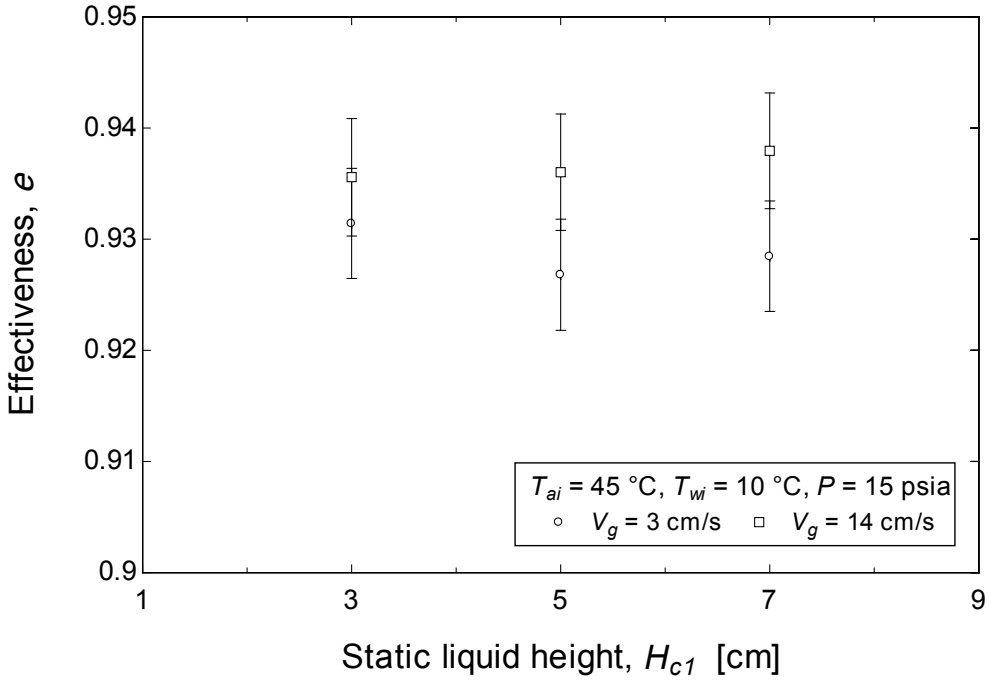

(b)

Figure 2-19 Effect of the static water column height on the total heat transfer rate (a) and effectiveness (b) in the bubble column dehumidifier

Figure 2-20 shows the effect of superficial velocity on the total heat transfer rate and effectiveness for the bubble column dehumidifier. In addition, the variation of the mass transfer coefficient with the superficial velocity is illustrated in Figure 2-21. It is evidently shown from Figure 2-20a that the total heat transfer rate significantly increases with the superficial velocity. This is mainly due to the increase of the mass flow rate which increases the sensible heat. The effectiveness of the dehumidifier increases gradually with the superficial velocity as shown in Figure 2-20b. Based on the definition of the effectiveness given in Equation (2-34), the variation of the exit air temperature discussed previously controls the variation in the effectiveness. The exit air temperature decreases in the dehumidifier with the superficial velocity which leads to this variation in the effectiveness. Moreover, the variation of the effectiveness could be explained from the relationship with the *NTU* which will be discussed later. Figure 2-21 shows the variation of the mass transfer coefficient determined from the *NTU* correlations given by Equations (2-32) and (2-33). It is noticed that, the mass transfer coefficient increases with the superficial velocity at any operating pressure due to the increase of the turbulent dissipation rate in the column. This is consistent with the previous research studies [28,30,31] for the mass transfer coefficient.

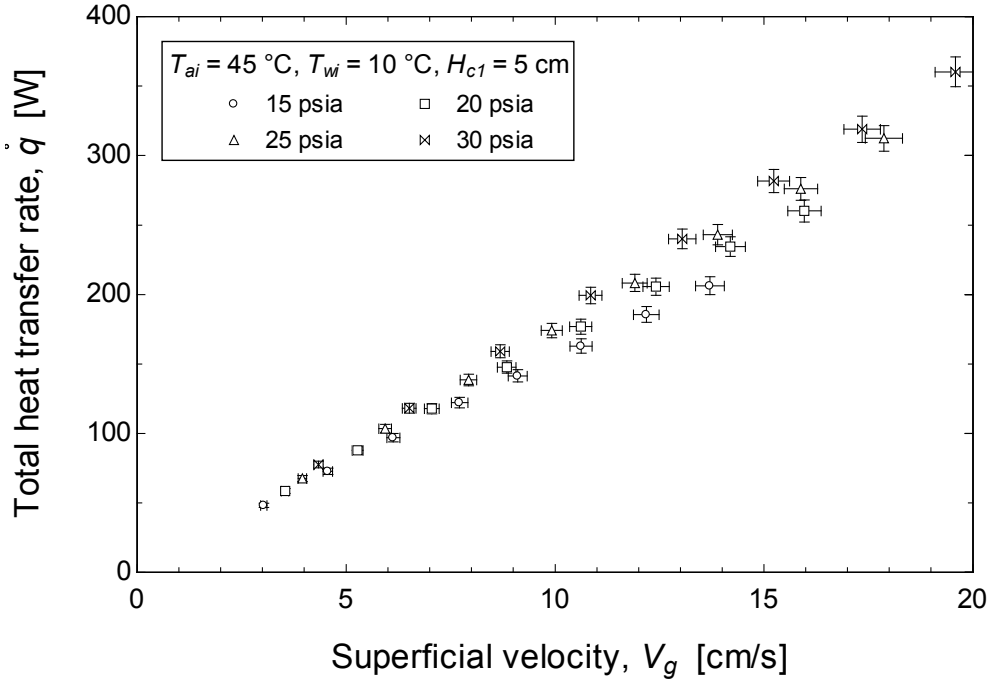

(a)

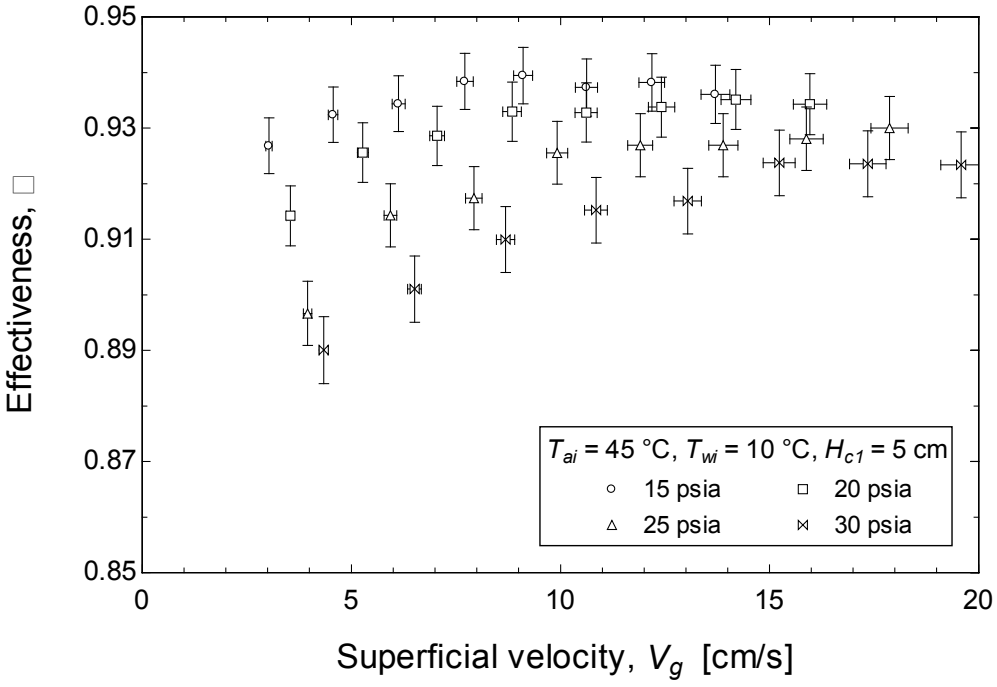

(b)

Figure 2-20 Effect of the superficial velocity and the pressure on the total heat transfer rate (a) and effectiveness (b) in the dehumidifier

The effect of pressure on the total heat transfer rate and effectiveness is shown in Figure 2-20 for the dehumidifier. The total heat transfer rate increases slightly with the pressure at values higher than the atmospheric pressure as shown in Figure 2-20a. This is because the increase of the pressure decreases the bubbles size and at the same time increases the gas holdup which again increases the specific area and the total heat transfer rate. On the other hand, the effectiveness of the dehumidifier decreases moderately with increasing pressure as shown in Figure 2-20b. Based on the ε-*NTU* model given by Equation (2-36) and the definition of the *NTU* given by Equation (2-32), the increase of the pressure leads to an increase in the air density for the same superficial velocity which consequently increases the air mass flow rate and reversely decreases the *NTU*. The decrease of *NTU* leads to the decrease in the effectiveness with the pressure.

Figure 2-21 shows the variation of the mass transfer coefficient in the dehumidifier. It is concluded from Figure 2-21 that increasing the pressure leads to the increase of mass transfer coefficient in the dehumidifier. This increase is more remarkable at higher superficial velocity. The effect of the pressure on the mass transfer coefficient in the case of the dehumidification process was discussed in a previous publication [31]. As the pressure increases, the bubbles size decreases which increase the gas holdup and the specific surface area which consequently increases the total heat transfer rate. Similar effect of the pressure on the bubble size and gas holdup was also observed by [28,30,31]. So it could be concluded here that the increase of the pressure generally increases the mass transfer coefficient in the dehumidification processes.

The ε-*NTU* model was developed by Braun et al. [19] for a cooling tower. However, a modified *HCR* of this model is given by Equation (2-35), and this model could be also used to model the bubble column dehumidifier. Since the heat and mass transfer processes are similar to what occurring in the cooling tower (with different energy direction and objective of the equipment). To validate this model, the experimental values of the *NTU* and effectiveness calculated by Equations (2-33) and (2-34) respectively are presented with the ε-*NTU* model as shown in Figure 2-22 for the dehumidifier.

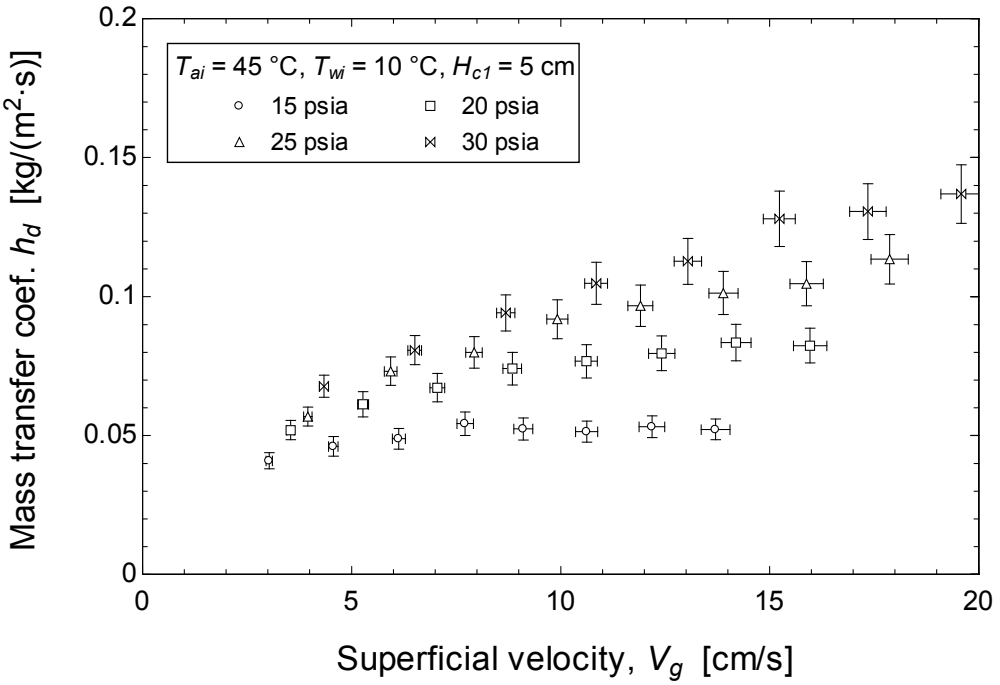

Figure 2-21 Effect of the superficial velocity and the pressure on the mass transfer coefficient in the dehumidifier

Figure 2-22 shows the relationship between the effectiveness and *NTU* for the dehumidifier. The *NTU* values are in a larger range between 6.8 and 9.4 because the entering air is hot and fully saturated with water vapor therefore the humidity ratio is higher and hence higher values of *NTU* is obtained from Equation (2-33). The minimum and maximum experimental values of *HCR* are 0.71 and 0.96 respectively. As shown in this figure, the *ε-NTU* model agrees well with the experimental results for the measured *NTU* range for the dehumidifier. Therefore, the variations of the effectiveness with respect to the pressure and superficial velocity as discussed previously could be described with the *ε-NTU* model which fits well the experimental data. The effect of pressure and superficial velocity on the effectiveness could be explained by analyzing the *NTU*.

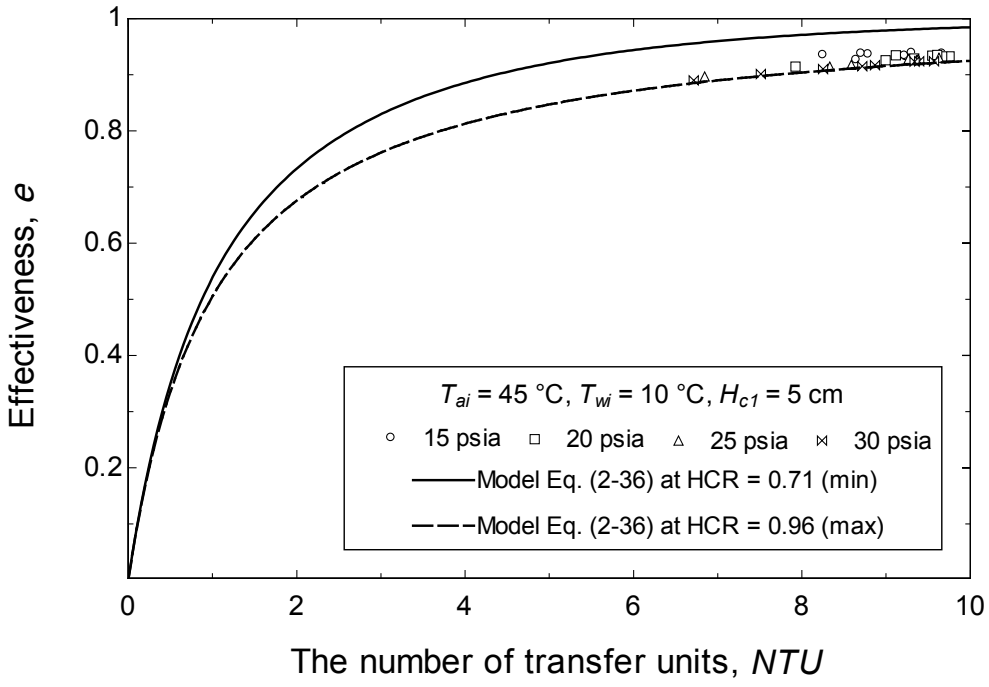

Figure 2-22 Experimental values of the effectiveness and *NTU* for the dehumidifier plotted with their corresponding model values given by Equation (2-36)

2.4 Chapter Conclusions

In this chapter, the pressure effect on the thermal performance of bubble column dehumidifier is investigated experimentally and theoretically based on two different operating conditions. For the constant column liquid temperature, a model is developed for the relationship between the effectiveness of the bubble column dehumidifier and the number of transfer units which combines the simultaneous heat and mass transfers occur inside the bubbles. This model ended with a relationship similar to that one for a heat exchanger with one fluid undergoing a phase change (or one fluid with a constant temperature). In addition, a model is modified for the mass transfer coefficient from the vapor into a vapor-gas mixture inside the bubble to capture the pressure effect. The model is presented with a correlation of Sherwood number as a function of Reynolds number, Schmidt number, and the density ratio. This model is calibrated using the experimental measurements conducted at different pressures and superficial velocities. For the constant inlet water temperature, a modified effectiveness-number of transfer units (ε-*NTU*) model for counter flow cooling tower is used to relate the experimental *NTU* and effectiveness values. The effect of the pressure, superficial velocity and liquid height in the column are discussed. The performance is evaluated by measuring the total heat transfer and the effectiveness.

The two ε-*NTU* models fit well with the experimental results, and the developed semi-empirical model predicates the total heat transfer rate and the effectiveness of the bubble column with a maximum deviation of 2% for both of them. It is found that the elevated pressure increases the total heat transfer rate but decreases the effectiveness. Besides,

increasing superficial velocities result in an increase of total heat transfer rate and the mass transfer coefficient in the dehumidifier. It is verified that the liquid height in the studied bubble column within the range of 3 – 7 cm, has no significant effect in the dehumidifier on the overall performance.

CHAPTER 3

BUBBLE COLUMN HUMIDIFIER

3.1 Mathematical Model

Figure 3-1 shows a schematic of the bubble column humidifier. It demonstrates the physical processes that take place in order to help presenting the thermal analysis. In the humidification process, cold air flows through a perforated plate at the bottom of the bubble column humidifier and distributed bubbles are generated in the column. The bubbles rise under the inertia and buoyancy forces, and contact directly with the warm water in the column. The inlet water temperature to the heating coil in the humidifier and the inlet air temperature are retained constant. However, the water temperature in the column varies according to the flow rate and operating pressure. Heat and mass transfer occur between the air and the water in the column due to the temperature and concentration differences. Consequently, the water in the column losses sensible heat that is compensated by the heating coil and it loses water molecule which are carried by the air as latent heat transfer.

Figure 3-2 shows a control volume that represents the humidification processes occur in the bubble column humidifier. The flow configuration of the circulated water inside the coil and the air in the bubble column can be treated as a counter flow heat exchanger. This is similar to the transport processes occur in a cooling tower where heat and mass are transferred between the air and water streams. In the following thermal analysis of the

bubble column humidifier, the inlet and outlet conditions are measured experimentally and the performance is calculated. The performance is evaluated by calculating the total heat transfer rate and effectiveness (ε). An ε-NTU model developed by Braun et al. [39] for counter flow cooling tower is used to determine the effective mass transfer coefficient in the bubble column. The derivation of the model for both cooling tower and bubble column should be the same. The difference between the two models is the surface area available for the simultaneous heat and mass transfer processes. In the cooling tower, this area is the surface area of the packing, however, in the bubble column it is the surface area of the bubbles in the column.

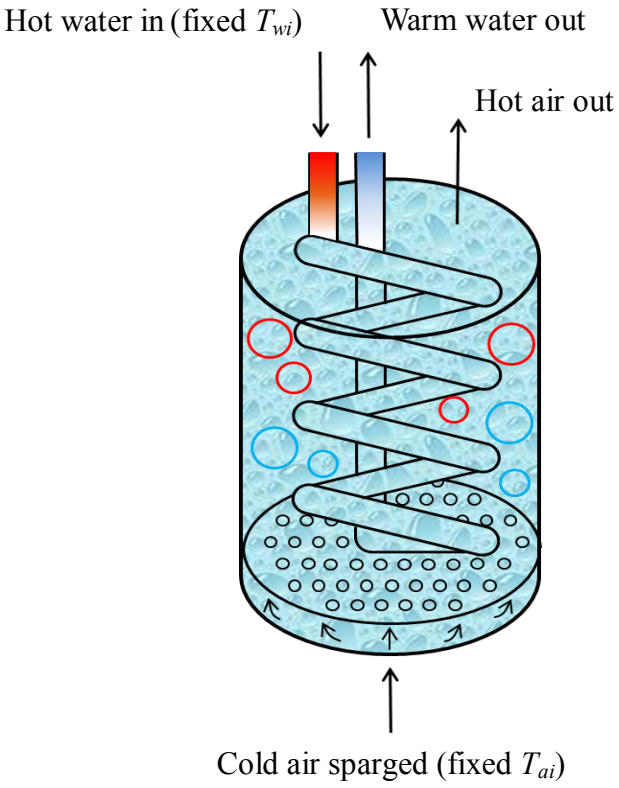

Figure 3-1 Schematic of the bubble column humidifier at constant T_{wi}

Applying an energy balance on the air and water streams of the control volume shown in Figure 3-2 for the humidifier,

$$d\dot{q}_a = d\dot{q}_w \tag{3-1}$$

The total heat transfer rate in the air and water sides can be expressed in terms of their total enthalpy changes,

$$d\dot{q}_a = \dot{m}_{da} di_a \tag{3-2}$$

$$d\dot{q}_w = -\dot{m}_w di_w \tag{3-3}$$

Contributing to the majority of the total heat transfer rate in the air stream, the latent heat transfer rate is respected to the increment of humidity ratio, and is shown as follows,

$$d\dot{q}_{lat} = \dot{m}_{da} i_{fg} d\omega_a \tag{3-4}$$

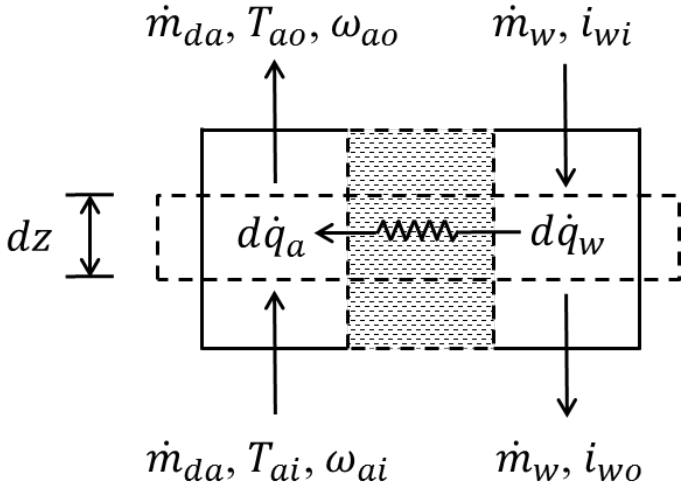

Figure 3-2 A finite volume element in a bubble column humidifier with a counter flow configuration

Analogous to a cooling tower, the mass balance over a finite volume is given by the following differential equation,

$$-d\omega_a = \frac{h_d a A_c}{\dot{m}_{da}}\left(\omega_a - \omega_{sa,w}\right)dz \tag{3-5}$$

Where h_d is defined as the convective mass transfer coefficient of the vapor diffusion into the bubbles. The number of transfer units (*NTU*) for a heat and mass exchanger is given by [39],

$$NTU = \frac{h_d a V_c}{\dot{m}_{da}} \tag{3-6}$$

Integrating Equation (3-5) and using the definition of *NTU* given by Equation (3-6), the following expression is obtained to calculate *NTU*.

$$NTU = \int_{\omega_{a,i}}^{\omega_{a,o}} \frac{d\omega_a}{(\omega_{sa,w} - \omega_a)} \tag{3-7}$$

The integration of Equation (3-7) is made by assuming a linear relationship between the humidity ratio of the saturated air and the water temperature since the variation in the water temperature is very small along the bubble column. The effectiveness is defined as the ratio of the actual total heat transfer rate to its maximum approaching value of the stream having minimum heat capacity. In the present work, the air stream has the minimum heat capacity and therefore an expression for its effectiveness is given by,

$$\varepsilon = \frac{i_{ao} - i_{ai}}{i_{sa,wi} - i_{ai}} \tag{3-8}$$

where $i_{sa,wi}$ is the enthalpy of saturated air at entering water temperature, which is the maximum possible temperature for the exit air in a counter flow heat exchanger.

The heat capacity ratio (*HCR*) for a heat and mass exchanger was modified by Narayan et al. [3,26]. It is defined as the ratio of maximum possible total enthalpy change between the cold stream and hot stream (*HCR* < 1),

$$HCR = min\left\langle \frac{i_{sa,wi}-i_{ai}}{i_{wi}-i_{w,ai}}, \frac{i_{wi}-i_{w,ai}}{i_{sa,wi}-i_{ai}} \right\rangle \tag{3-9}$$

Analogous to a counter flow heat and mass exchanger, the relationship of the effectiveness and *NTU* is given by Equation (3-10) [39],

$$\varepsilon = \frac{1-exp[-(1-HCR)\cdot NTU]}{1-HCR\cdot exp[-(1-HCR)\cdot NTU]} \tag{3-10}$$

In order to determine the mass transfer coefficient from Equation (3-6), the specific area (a) in the bubble column is required. The specific area is given by Equation (3-11) assuming that the bubbles are of mean sauter diameter [40],

$$a = \frac{6\epsilon}{d_b} \tag{3-11}$$

The gas holdup in Equation (3-11) is given by the following expression provided by Joshi and Sharma [45],

$$\epsilon = \frac{V_g}{0.3+2V_g} \tag{3-12}$$

where V_g is the superficial velocity calculated by dividing the actual air flow rate by the cross-sectional area of the bubble column. The gas holdup (ϵ) can be also expressed by

the following relationship which relates the aerated liquid height in the bubble column (H_{c2}), to the static liquid height (H_{c1}), provided by Akita and Yoshida [41].

$$\epsilon = \frac{H_{c2}-H_{c1}}{H_{c2}} \tag{3-13}$$

The aerated liquid height (H_{c2}) is used to determine the aerated volume (Vc) which appears in Equation (3-6) by multiplying it by the cross-sectional area (A_c).

Finally, the following expression given by Miller [40] and Narayan et al. [11] in a similar system is used to determine the bubble mean diameter.

$$d_b = \left[\frac{6\sigma d_o}{(\rho_w-\rho_a)g}\right]^{1/3} \tag{3-14}$$

The convectional ε-*NTU* model in the counter flow heat transfer is novel to be used in the bubble column humidifier (to the authors' best knowledge). For a design purpose, giving the required conditions of heat exchanger, the value of the *NTU* can be determined as a demand of geometrical parameters. For a performance elevation, the effectiveness and outlet conditions of air and water can be solved with known parameters of the *NTU* and inlet conditions of air and water. However, for design purpose, we should know the convective mass transfer coefficient h_d in order to calculate *NTU* for a given bubble column geometry. In Section 3.3, the experimental data will be presented and the *NTU* relationships given by Equations (3-6) and (3-7) will be used to determine the mass transfer coefficient. In addition, the ε-*NTU* model will be presented with the experimental values of the effectiveness and *NTU* to demonstrate that it is a good working model which could be used to predict the effectiveness of the bubble column humidifier or

dehumidifier at different operating conditions. Therefore, it could be utilized in the design or the performance evaluation of bubble columns.

The set of equations in the mathematical model are modeled and solved numerically by using a computer program Engineering Equation Solver (EES) [46]. The physical properties of moist air and liquid water are acquired from its built-in functions relying on good accuracy thermodynamic and transport properties database. The non-linear equations are solved iteratively to obtain the outputs of performance evaluations based on the inputs of operating conditions, with graphic solutions generated in plots.

3.2 Experimental Work

3.2.1 Experimental Setup

A schematic of the experimental setup (see Figure 3-3) provides the main components and the basic flow paths in the humidifier test. For the bubble column humidifier tests under reduced pressure, the air flows through the dehumidifier first where it is cooled and dehumidified then through the humidifier where it is heated and humidified. A vacuum pump (30) is connected to the exit of the humidifier where the air is sucked and a sub-atmospheric pressure is created inside the system. The pressure and flow rates are controlled by a set of valves (1, 8, 11, 16, 23, and 26). The bubble columns are filled with water to a certain level and the temperature of the water in the columns is controlled by heating and cooling coils inserted inside the humidifier and dehumidifier respectively.

Both bubble columns have perforated plates (3, 18) at its bottom where air is sparged through its holes and bubbles aerate the columns.

The structure and geometry of both bubble columns are the same. The external body of the bubble columns is made of transparent PVC tubes of 100 mm inside diameter, 10 mm thickness, and 250 mm height. The tubes are enclosed by two cover plates at the top and bottom where the air inlet and exit ports as well as the measuring instruments are connected. The external surface of the columns was insulated by glass wool blanket of 5 cm thickness to reduce the heat loss or gain to or from the surroundings. A copper coil is installed inside each bubble column to provide the heating or cooling load needed during the experiments. The copper coils have an outside diameter of 9.5 mm, a wall thickness of 0.9 mm, and is spiraled to a helical height of 90 mm with a turn outside diameter of 98 mm. Hot and cold waters are circulated inside the coil in the humidifier and dehumidifier respectively. A water chiller (12) (Thermal Scientific model Accel 500 LC) is connected to the cooling coil installed inside the dehumidifier which provide a cooling capacity up to 500 W and a temperature range of 0 – 80 °C. The heating coil in the humidifier is connected to a constant temperature circulating bath (27) (Omega model HCTB-3010) which provides a heating capacity up to 1000 W and an adjustable temperature range of 20 – 95 °C.

The air is sparged through the perforated plates (3, 18) installed at the bottom of each bubble column which distribute the air and generate bubbles. The perforated plate consists of a stainless steel cylindrical box of 98 mm outside diameter and 18 mm height. A plate covers this box and has 83 holes of 1 mm diameter each drilled in a staggered distribution with a pitch of 9 mm. The air enters at the bottom of the perforated plate box

through stainless steel tube and hose. During the experimental tests, the perforated plate and fittings causes a maximum pressure drop of a 0.12 bar (1.7 psia) at the highest flow rate tested. The level of water in the bubble column is adjusted using make-up tanks (9, 24) which are connected to the bottom of each bubble column.

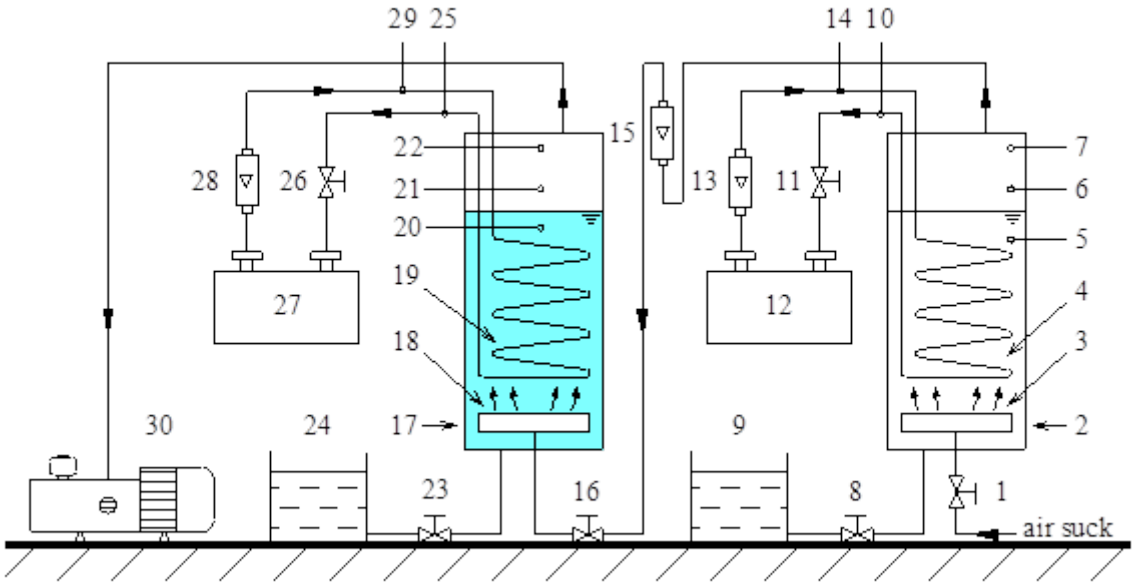

Figure 3-3 Schematic of the experimental setup for humidifier test at fixed T_{wi}
(1, 8, 11, 16, 23, 26) valve, (2) bubble column dehumidifier, (3, 18) perforated plates, (4, 19) copper coils, (5, 6, 10, 14, 20, 21, 25, 29) thermocouples, (7, 22) absolute pressure sensors, (9, 24) make-up tanks, (12) water chiller, (13, 15, 28) rotameter, (17) bubble column humidifier, (27) water heater, (30) vacuum pump

The operating parameters of flow rate, temperature, and pressure are measured using rotameters (13, 15, 28), thermocouples (5, 6, 10, 14, 20, 21, 25, 29) and absolute pressure gauges (7, 22) respectively. The air flow rate is measured using the rotameter (15) which has a range of 0.5 – 4.5 ft^3/min (236 – 2124 cm^3/s) and an uncertainty of ±2.5%. The water flow rates in the cooling and heating coils are measured using rotameters (13, 28) which have a range of 0.8 – 8 L/min.

All thermocouples are of K-type connected to a 12-channel temperature logger (Omega, RDXL 12SD). The thermocouples and the data logger system have a combined uncertainty of ±0.25 K. The absolute pressure of the air inside the bubble columns is measured by digital pressure gauges (Omega, DPG1000B-100A) which have a range of 0 – 100 psia (0 – 6.89 bar absolute) and an uncertainty of ±0.1 psia ($\pm 6.89 \times 10^{-3}$ bar). The water level in the columns is measured directly by a ruler attached to the outside surface of the bubble columns. The hydrostatic pressure of the liquid in column and the pressure drop in the perforated plate are considered in the measured pressure during the humidifier test. The absolute pressure of moist air in the rotameter which determines its density is obtained from the pressure measurements of humidifier (22) and dehumidifier (7) along with total pressure drop mentioned above.

3.2.2 Experimental Procedure

Before the experimental test starts, gas leakage test is performed to avoid any air leakage from the system. The temperatures from all thermocouples are checked before the implementation of any heating or cooling loads to guarantee a uniform temperature

environment. Every run is accomplished to when a steady state condition is achieved at which all measuring variables fluctuate within their uncertainty tolerances, and continuously carried out for new experimental set conditions.

In the humidifier test, water level in the bubble column humidifier was adjusted to the desired level (3, 5, or 7 cm) using the make-up tank (24). Similarly, the water level in the dehumidifier was fixed at 5 cm using the make-up tank (9). During the humidifier experimental run, the inlet water temperature to the heating coil in the humidifier was fixed at 45 °C, and the inlet air temperature to the humidifier was fixed at 15 °C by adjusting the water column temperature in the dehumidifier. The air flow rate through the humidifier was adjusted by the control valve (16) while the humidifier pressure was adjusted by a pressure regulator on the vacuum pump. The reduced pressures in the humidifier were set to 7 psia (0.48 bar), 8 psia (0.55 bar), 10 psia (0.69 bar) and 12 psia (0.83 bar). We could not achieve higher flow rates at lower pressures because of the limiting flow capacity of the vacuum pump. Therefore, in the experimental results, there are few superficial velocities at lower pressures. For comparison, an atmospheric condition at nearly 15 psia (1.03 bar) is given by removing the vacuum pump (30) with its pipe and supplying an air compressor to the front end of the valve (1). Along a simultaneous change with the varying pressure, the air flow rate measured in the rotameter (15) determines the superficial velocity in a total range of 2 – 16 cm/s.

3.2.3 Calibration and Uncertainty Analysis

To improve the precision of the measurements, a careful calibration of all instruments was performed and the measured data was compared with standard values. The thermocouples were calibrated with a liquid-in-glass thermometer which has a 0.1 K least count while the pressure transducers were calibrated using a dead weight tester to ensure that their readings are accurate to the standard values provided by the manufacturers.

The flow rate measured by the rotameter is corrected due to the difference in the moist air density from the dry air at the STP condition (Standard Temperature and Pressure) for which it was calibrated by the manufacturer. Since the air flow in the rotameter is mainly inviscid, the flow rate is proportional to the square root of the air density. Therefore, a correction to the air flow rate is given by Equation (3-15). On the other hand, the rotameter was installed at the humidifier exit where cold air flows through to reduce the effect of condensation.

$$\frac{\dot{V}_{a,m}}{\dot{V}_a} = \sqrt{\frac{\rho_{a,STP}}{\rho_{ai}}} \tag{3-15}$$

The uncertainty mainly arises from the instruments, experiment condition, and observations of measured quantities. Uncertainty analysis is essential to evaluate the accuracy of each calculated result. In this work, the uncertainty of the calculated results is determined using the method described by Coleman and Steele [47]. Based on the uncertainty of each instrument previously stated in Section 3.2.1, the uncertainty of each calculated parameter is determined using the uncertainty propagation function in EES commercial software [46]. The uncertainty bars are shown in the results figures that are presented in Section 3.3.

3.3 Results and Discussion

3.3.1 The Air and Water Outlet Temperatures

Experimental measurements are conducted for the bubble column humidifier under different operating conditions. The parameters that are varied in the experimental runs are the static liquid height, superficial velocity, and pressure. However, the inlet temperatures of both air and water are fixed for the bubble column humidifier. The thermal performance of the bubble column is presented by calculating the total heat transfer rate and the effectiveness. In addition, the mass transfer coefficient is illustrated under varying superficial velocity and pressure.

Figure 3-4 shows the outlet temperatures of air and water in the humidifier at sub-atmospheric pressures and different superficial velocities. The exit air temperature and exit water temperature both decrease with the increase of the superficial velocity. The decrease of the exit air temperature could be attributed to the increase of the heat transfer coefficient with increasing the superficial velocity due to the enhanced turbulence [15]. The decrease of the exit air temperature with the superficial velocity could be also explained from the decrease of the *NTU* with the air flow rate which consequently decreases the air effectiveness (see Figure 3-8). On the other hand, the increase of the air flow rate directly increases the sensible heat transfer rate which leads to a decrease of the exit water temperature since the water flow rate and inlet water temperature are both fixed.

The effect of pressure on the outlet air and water temperatures in the humidifier is also shown in Figure 3-4. In the humidifier, it is concluded that the exit air temperature is

slightly increases when the pressure is reduced to sub-atmospheric values at a given superficial velocity. The slight increase of the exit air temperature could be explained by the decrease in the mass transfer coefficient with the pressure as will be shown in Figure 3-7. On the other hand, the exit water temperature in the humidifier is found insignificantly affected by the pressure, not surprising that the exit air temperature in the humidifier is slightly increased at a reduced pressure.

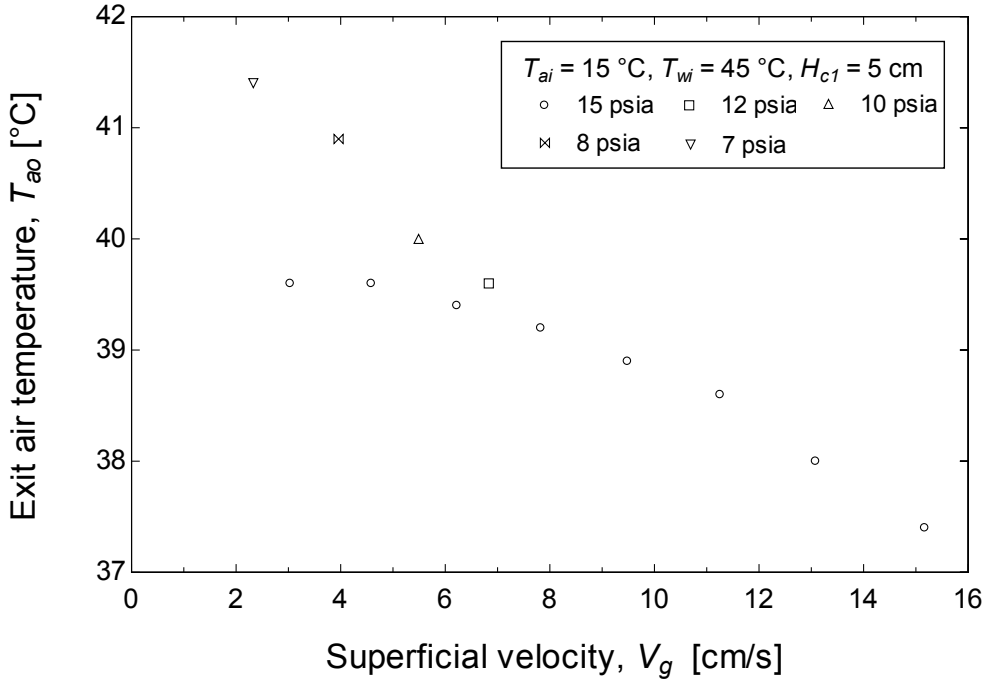

(a)

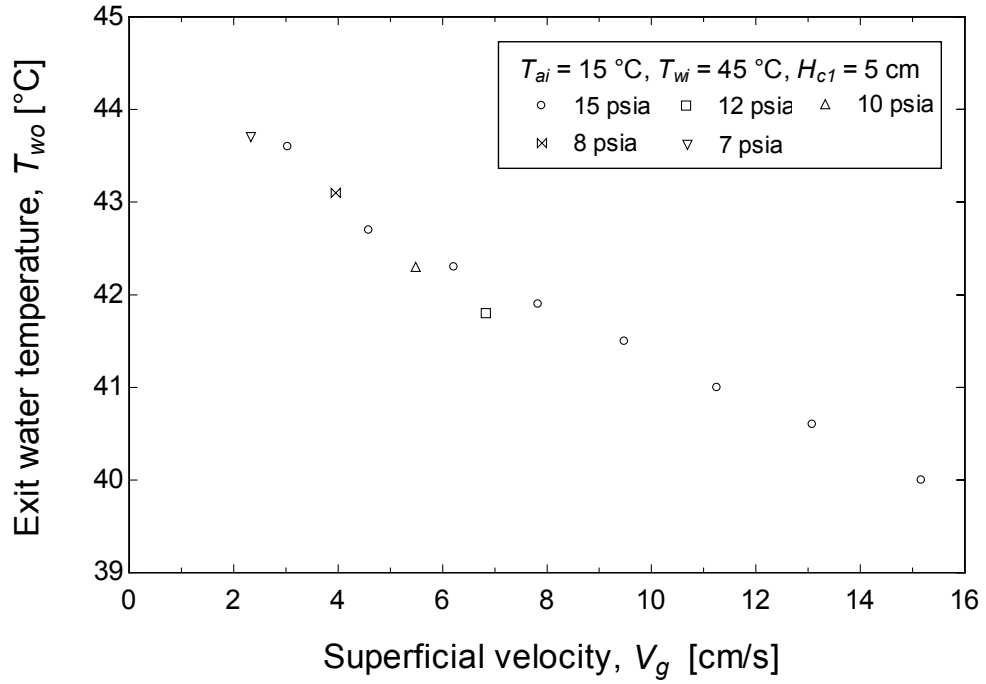

(b)

Figure 3-4 Outlet temperatures of air (a) and water (b) in the bubble column humidifier at different pressures and superficial velocities

3.3.2 Effect of Column Liquid Height

The column liquid height discussed herein is the static height of the water in the column. During the experimental runs, we varied the static height in the range of 3 – 7 cm which does not immerse the coil totally. However, the aerated liquid height after bubbling effectively covered the coil. It was not possible to increase the static liquid height more than 7 cm as there is no much space and the water in the column will flow with the air stream. The influences of varying the column liquid height on the total heat transfer rate and effectiveness for humidifier case were determined. As shown in Figure 3-5, the effect of column liquid height in the humidifier is found insignificant to either the total heat transfer rate or the effectiveness which agrees well with these previous studies [11,12,31]. Accordingly, the remaining experimental results exclude the liquid height effect and will show all humidifier tests at a liquid height of 5 cm.

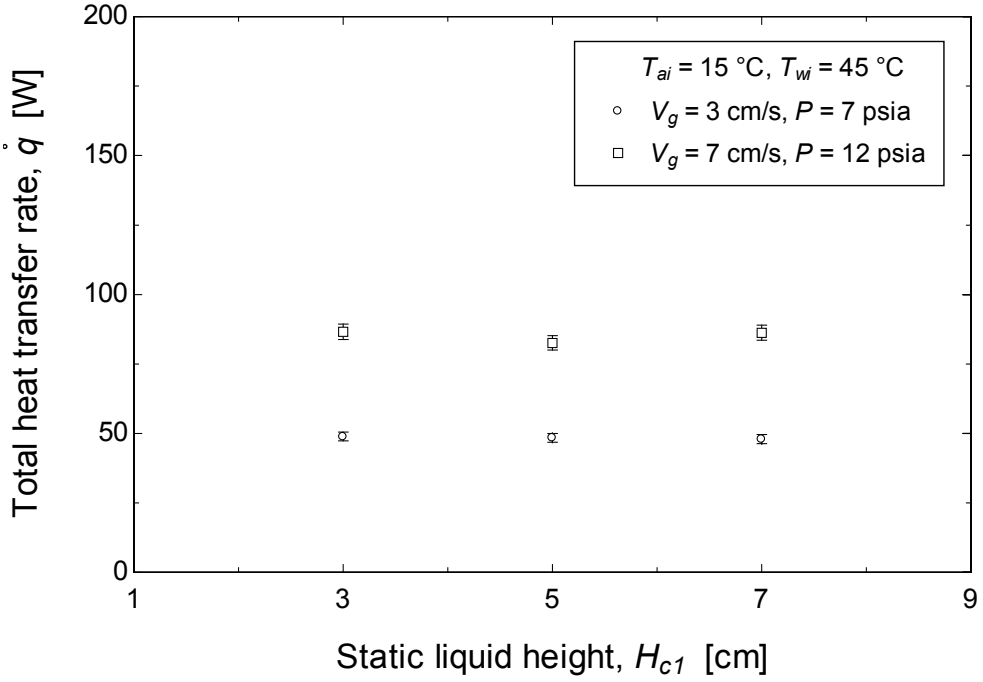

(a)

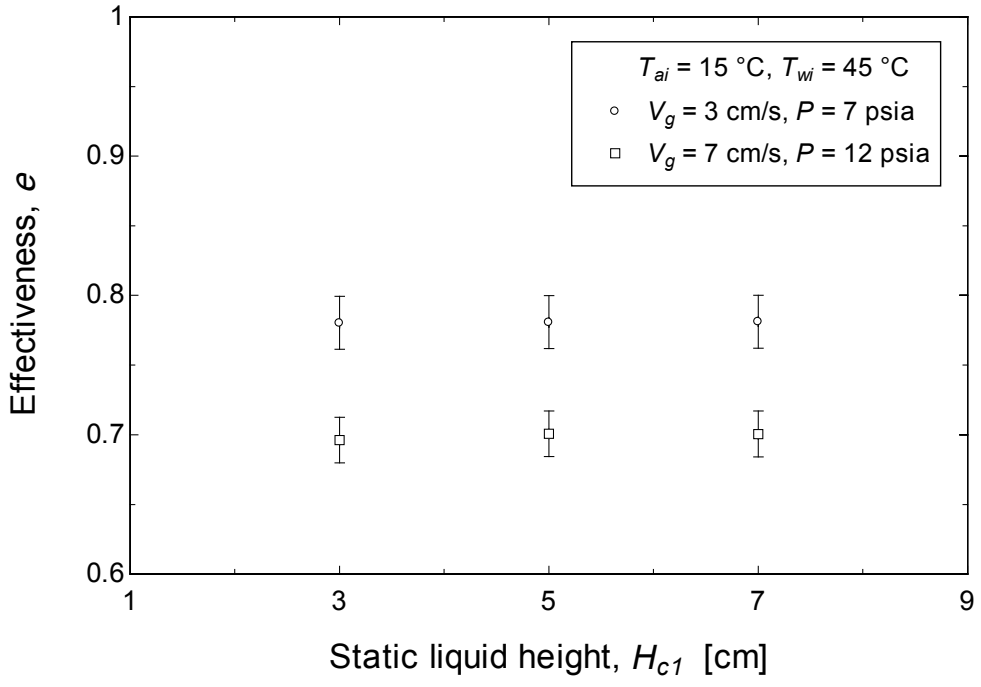

(b)

Figure 3-5 Effect of static water column height on the total heat transfer rate (a) and effectiveness (b) in the bubble column humidifier

3.3.3 Effect of Superficial Velocity

Figure 3-6 shows the effect of superficial velocity on the total heat transfer rate and effectiveness for the bubble column humidifier. In addition, the variation of the mass transfer coefficient with the superficial velocity is illustrated in Figure 3-7. It is evidently shown from Figure 3-6a that the total heat transfer rate significantly increases with the superficial velocity. This is mainly due to the increase of the mass flow rate which increases the sensible heat. The effectiveness of the humidifier decreases significantly with the superficial velocity as shown in Figure 3-6b. Based on the definition of the effectiveness given in Equation (3-8), the variation of the exit air temperature discussed in Section 3.3.1 controls the variation in the effectiveness. As discussed in 3.3.1, the exit air temperature decreases in the humidifier with the superficial velocity which leads to this variation in the effectiveness. Moreover, the variation of the effectiveness could be explained from the relationship with the *NTU* which will be discussed in Section 3.3.5. Figure 3-7 shows the variation of the mass transfer coefficient determined from the *NTU* correlations given by Equations (3-6) and (3-7). It is noticed that, the mass transfer coefficient increases with the superficial velocity at any operating pressure due to the increase of the turbulent dissipation rate in the column. This is consistent with the previous research studies [28,30,31] for the mass transfer coefficient.

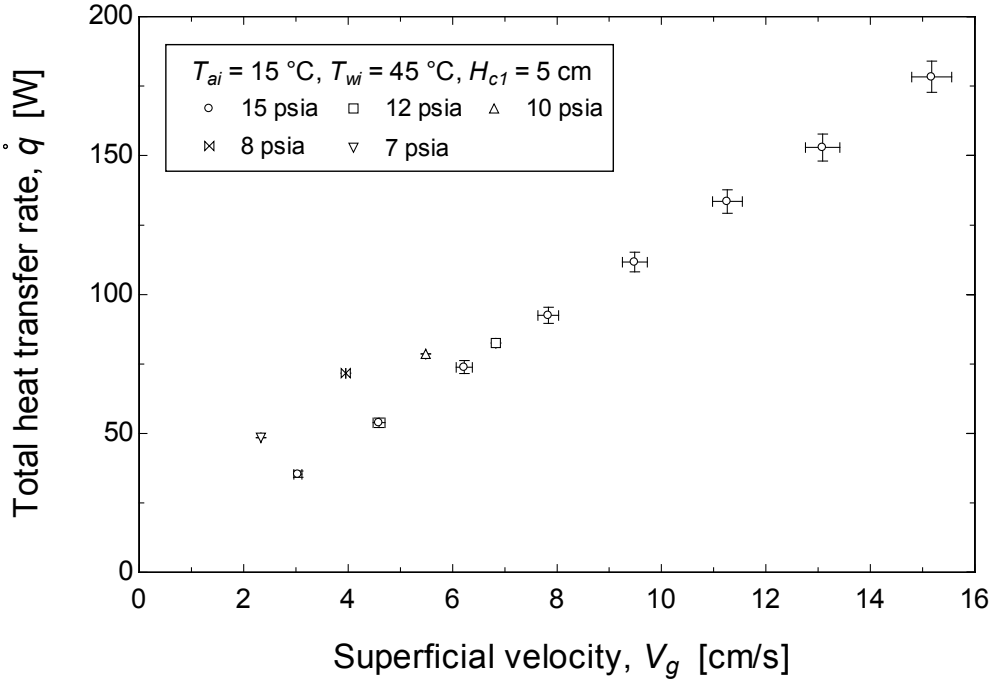

(a)

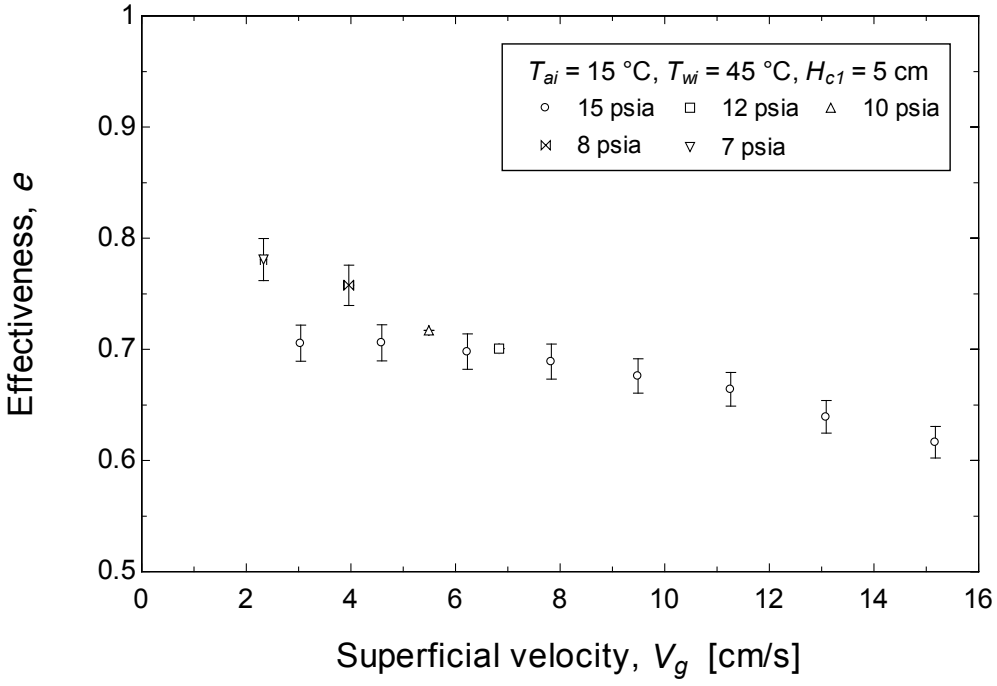

(b)

Figure 3-6 Effect of the superficial velocity and the pressure on the total heat transfer rate (a) and effectiveness (b) in the humidifier

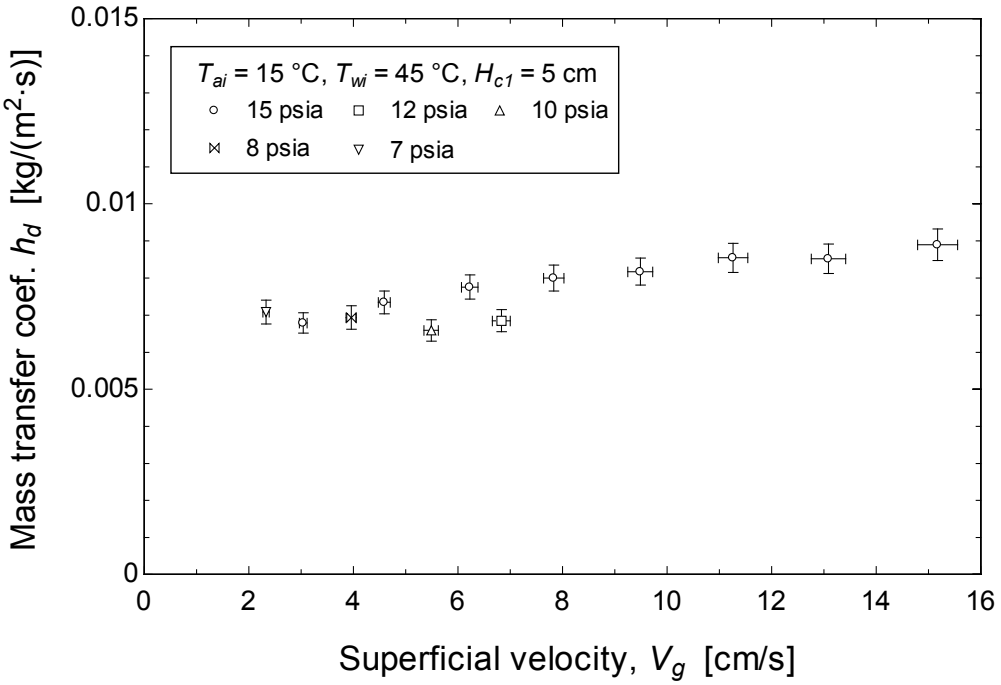

Figure 3-7 Effect of the superficial velocity and the pressure on the mass transfer coefficient in the humidifier

3.3.4 Effect of Pressure

The effect of pressure on the total heat transfer rate and effectiveness is shown in Figure 3-6 for the humidifier. Decreasing the pressure to sub-atmospheric values slightly increases the total heat transfer rate as shown in Figure 3-6a. This indicates that decreasing the pressure to the sub-atmospheric value enhance the humidification process and allow more water vapor molecule to transfer to the air stream. In addition, as the pressure decreases in the humidifier the effectiveness increases slightly as shown in Figure 3-6b. This could be explained by the increase of the mass transfer coefficient which consequently increases the exit air temperature.

Figure 3-7 shows the variation of the mass transfer coefficient in the humidifier. It is concluded from Figure 3-7 that increasing the pressure leads to the increase of mass transfer coefficient in the humidifier. This increase is more remarkable at higher superficial velocity. The effect of the pressure on the mass transfer coefficient in the case of the dehumidification process was discussed in a previous publication [14]. As the pressure increases, the bubbles size decreases which increase the gas holdup and the specific surface area which consequently increases the total heat transfer rate. Similar effect of the pressure on the bubble size and gas holdup was also observed by [28,30,31]. So it could be concluded here that the increase of the pressure generally increases the mass transfer coefficient in the humidification processes.

3.3.5 The Use of *ε–NTU* Model

The *ε-NTU* model was developed by Braun et al. [39] for a cooling tower. However, a modified *HCR* of this model is given by Equation (3-9), and this model could be also used to model the bubble column humidifier. Since the heat and mass transfer processes are similar to what occurring in the cooling tower (with different energy direction and objective of the equipment). To validate this model, the experimental values of the *NTU* and effectiveness calculated by Equations (3-7) and (3-8) respectively are presented with the *ε-NTU* model as shown in Figure 3-8 for the humidifier.

Figure 3-8 shows the experimental values of the *ε* and *NTU* for the humidifier at all superficial velocities and pressures. In addition, the *ε-NTU* model is plotted in the same figure at *HCR* values corresponding to the minimum and maximum experimental values calculated by Equation (3-9). As shown in the figure, the *ε-NTU* model agrees well with the experimental results for the measured *NTU* range of 1.1 – 2.1. The change of the *NTU* is mainly due to the variation of the air mass flow rate due to the changes of the superficial velocity and the air density (the density changes due to the pressure variation). Consequently, the effectiveness increases with the superficial velocity. Therefore, the variations of the effectiveness with respect to the pressure and superficial velocity as discussed previously could be described with the *ε-NTU* model which fits well the experimental data. The effect of pressure and superficial velocity on the effectiveness could be explained by analyzing the *NTU*.

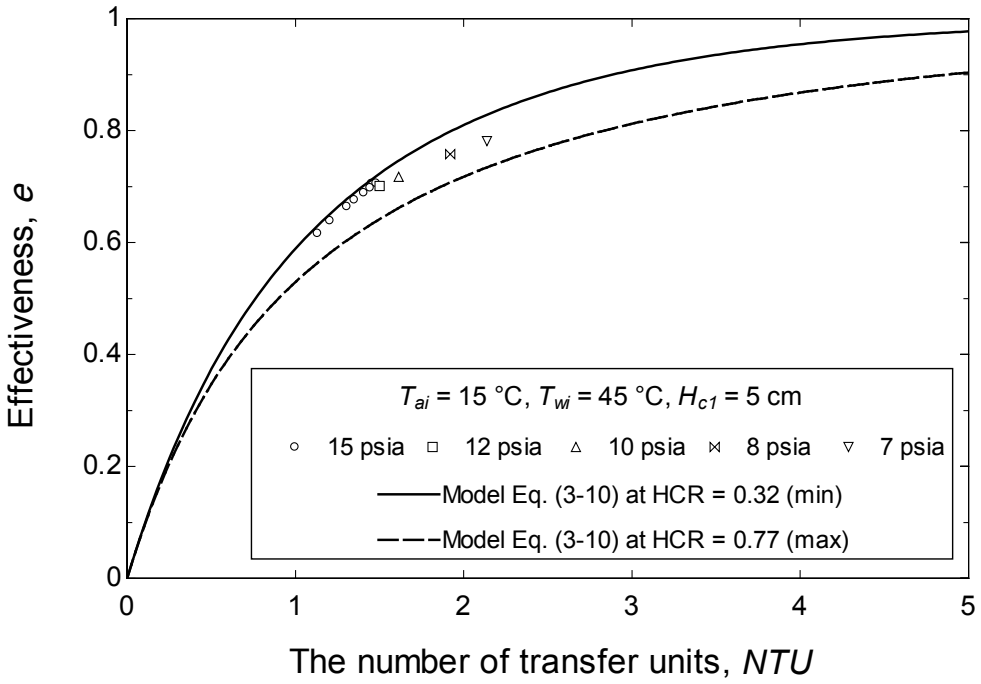

Figure 3-8 Experimental values of the effectiveness and *NTU* for the humidifier plotted with their corresponding model values given by Equation (3-10)

3.4 Chapter Conclusions

In this chapter, the pressure effect on the thermal performance of bubble column humidifier is investigated based on experimental work. The sub-atmospheric pressure is operated, and the inlet temperatures of air and water are fixed. The other operating conditions comprise of superficial velocity and column liquid height. The performance is evaluated by measuring the total heat transfer and the effectiveness. An ε-*NTU* model for counter flow heat and mass exchanger is employed combined with thermal analysis between the air and water streams.

The modified ε-*NTU* model agrees well with the experimental values of the effectiveness and *NTU* for the humidifier. The experimental results show that under the sub-atmospheric pressure, the lower pressure is advantageous to both the heat transfer rate and the effectiveness. Therefore, it is recommended to operate lower pressure in the bubble column humidifier. It is demonstrated that the liquid height in the column has no significant effect on the performance however; the superficial velocity increases both the heat transfer and effectiveness for the humidifier.

CHAPTER 4

CONCLUSIONS AND RECOMMENDATIONS

4.1 Conclusions

In the present work, the effect of the pressure on the bubble column humidifier and dehumidifier is investigated experimentally and theoretically under different operating conditions.

For the dehumidifier test under constant column liquid temperature, the effect of the pressure on the dehumidification process of bubble column dehumidifier is investigated. A model is developed for the relationship between the effectiveness of the bubble column dehumidifier and the number of transfer units which combines the simultaneous heat and mass transfers occur inside the bubbles. This model ended with a relationship is similar to that one for a heat exchanger with one fluid undergoing a phase change (or one fluid with a constant temperature). In addition, a model is modified for the mass transfer coefficient from the vapor into a vapor–gas mixture inside the bubble to capture the pressure effect. The model is presented with a correlation of Sherwood number as a function of Reynolds number, Schmidt number, and the density ratio. This model is calibrated using the experimental measurements conducted at different pressures and superficial velocities.

For the dehumidifier and humidifier under constant inlet water temperatures, the pressure effect on the thermal performance of bubble column humidifier and dehumidifier is

investigated experimentally. In addition, the effect of the superficial velocity and liquid height in the column are discussed. The performance is evaluated by measuring the total heat transfer and the effectiveness. Moreover, an ε-*NTU* model is used to relate the experimental *NTU* and effectiveness values.

The main obtained results are summarized as follows:

- It is verified that there is no significance for the liquid height in either humidifier or dehumidifier to the overall performance.
- Higher superficial velocities result in an increase of total heat transfer rate and the mass transfer coefficient in both the bubble column humidifier and dehumidifier. However, the effectiveness in the humidifier is decreased, compared to the dehumidifier effectiveness which increases with the superficial velocity.
- For the humidifier under the sub-atmospheric pressure, the lower pressure is advantageous to both the heat transfer rate and the effectiveness. For the dehumidifier under the elevated pressure, the higher pressure is beneficial for the heat transfer rate, but against the effectiveness.
- The modified ε-*NTU* model based on the counter flow cooling tower agrees well with the experimental values of the effectiveness and *NTU* for both the humidifier and dehumidifier.
- The developed model of Sherwood number predicts the total heat transfer rate and the effectiveness of the bubble column with a maximum deviation of 2% for both of them.

4.2 Recommendations

It has been demonstrated that the pressure has considerable effects on the humidification and dehumidification processes in bubble columns. However, combining the advantages of the entire pressure effect on the complete HDH system with the usage of bubble column humidifier and dehumidifier needs further investigation.

Overall, some recommendations are provided for any future work:

- It is suggested to operate a bubble column HDH system under lower humidifier pressure. However, it is not recommended to operate higher pressure in the dehumidifier since it requires a larger dehumidifier size to compensate for the decrease occurs in the effectiveness.
- The effect of the column liquid height on the gas holdup needs further investigation for bubble columns with lower aspect ratio (height to diameter).
- In the humidifier test under sub-atmospheric pressure, a varying superficial velocity in a fixed reduced pressure is requested to obtain more experimental results for further analysis.
- Measurements for the productivity and input energy are necessary for more parametric investigations in the future complete bubble column HDH cycle.
- Some improved designs are expected to provide more effective, reliable and economic in practical applications. For example, a solution is need for the flexible water volume control in the closed bubble column when operated under higher or lower absolute pressure, less copper coil material is used, different dimensions of bubble column with varying aspect ratio is applied, etc.

REFERENCES

[1] Sharqawy, M. H., Antar, M. A., Zubair, S. M., and Elbashir, A. M., 2014, "Optimum thermal design of humidification dehumidification desalination systems," Desalination, **349**, pp. 10–21.

[2] Antar, M. A., and Sharqawy, M. H., 2013, "Experimental investigations on the performance of an air heated humidification–dehumidification desalination system," Desalin. Water Treat., **51**(4-6), pp. 837–843.

[3] Narayan, G. P., Mistry, K. H., Sharqawy, M. H., Zubair, S. M., and Lienhard V, J. H., 2010, "Energy effectiveness of simultaneous heat and mass exchange devices," Front. Heat Mass Transf., **1**, pp. 1–13.

[4] Narayan, G. P., Sharqawy, M. H., Summers, E. K., Lienhard, J. H., Zubair, S. M., and Antar, M. A., 2010, "The potential of solar-driven humidification–dehumidification desalination for small-scale decentralized water production," Renew. Sustain. Energy Rev., **14**(4), pp. 1187–1201.

[5] Dai, Y. J., Wang, R. Z., and Zhang, H. F., 2002, "Parametric analysis to improve the performance of a solar desalination unit with humidification and dehumidification," Desalination, **142**(2), pp. 107–118.

[6] Yamali, C., and Solmus, I., 2008, "A solar desalination system using humidification-dehumidification process: experimental study and comparison with the theoretical results," Desalination, **220**(1-3), pp. 538–551.

[7] Yuan, G., Wang, Z., Li, H., and Li, X., 2011, "Experimental study of a solar desalination system based on humidification–dehumidification process," Desalination, **277**(1-3), pp. 92–98.

[8] Khedr, M., 1993, "Techno-Economic investigation of an air humidification-dehumidification desalination process," Chem. Eng. Technol., **16**(4), pp. 270–274.

[9] Chafik, E., 2003, "A new type of seawater desalination plants using solar energy," Desalination, **156**(1-3), pp. 333–348.

[10] Müller-Holst, H., 2007, "Solar thermal desalination using the multiple effect humidification (MEH) method," Solar Desalination for the 21st Century, Springer, Dordrecht, pp. 215–225.

[11] Narayan, G. P., Sharqawy, M. H., Lam, S., Das, S. K., and Lienhard V, J. H., 2013, "Bubble columns for condensation at high concentrations of noncondensable gas: Heat-transfer model and experiments," AIChE J., **59**(5), pp. 1780–1790.

[12] Tow, E. W., and Lienhard V, J. H., 2014, "Experiments and modeling of bubble column dehumidifier performance," Int. J. Therm. Sci., **80**, pp. 65–75.

[13] El-Agouz, S. A., and Abugderah, M., 2008, "Experimental analysis of humidification process by air passing through seawater," Energy Convers. Manag., **49**(12), pp. 3698–3703.

[14] El-Agouz, S. A., 2010, "Desalination based on humidification–dehumidification by air bubbles passing through brackish water," Chem. Eng. J., **165**(2), pp. 413–419.

[15] Kantarci, N., Borak, F., and Ulgen, K. O., 2005, "Bubble column reactors," Process Biochem., **40**(7), pp. 2263–2283.

[16] Urseanu, M. I., 2000, "Scaling up bubble column reactors," Ph.D thesis, University of Amsterdam.

[17] Zehner, P., and Kraume, M., 2000, "Bubble columns," Ullmann's Encyclopedia of Industrial Chemistry, Wiley Online Library, Weinheim, Germany.

[18] Shaikh, A., and Al-Dahhan, M. H., 2007, "A review on flow regime transition in bubble columns," Int. J. Chem. React. Eng., **5**.

[19] Tow, E. W., and Lienhard V, J. H., 2014, "Heat transfer to a horizontal cylinder in a shallow bubble column," Int. J. Heat Mass Transf., **79**, pp. 353–361.

[20] Vlachogiannis, M., Bontozoglou, V., Georgalas, C., and Litinas, G., 1999, "Desalination by mechanical compression of humid air," Desalination, **122**(1), pp. 35–42.

[21] Higbie, R., 1935, "The rate of absorption of a pure gas into a still liquid during a short time of exposure," Trans. AIChE, **31**, pp. 365–389.

[22] Kang, Y. T., Akisawa, A., and Kashiwagi, T., 2000, "Analytical investigation of two different absorption modes: falling film and bubble types," Int. J. Refrig., **23**(6), pp. 430–443.

[23] Mori, Y., and Nakayama, W., 1965, "Study on forced convective heat transfer in curved pipes (1st report, laminar region)," Int. J. Heat Mass Transf., **8**(1), pp. 67–82.

[24] Deckwer, W.-D., 1980, "On the mechanism of heat transfer in bubble column reactors," Chem. Eng. Sci., **35**(6), pp. 1341–1346.

[25] Ghazal, M. T., Atikol, U., and Egelioglu, F., 2014, "An experimental study of a solar humidifier for HDD systems," Energy Convers. Manag., **82**, pp. 250–258.

[26] Narayan, G. P., Sharqawy, M. H., Lienhard V, J. H., and Zubair, S. M., 2010, "Thermodynamic analysis of humidification dehumidification desalination cycles," Desalin. Water Treat., **16**(1-3), pp. 339–353.

[27] Ghalavand, Y., Hatamipour, M. S., and Rahimi, A., 2014, "Humidification compression desalination," Desalination, **341**, pp. 120–125.

[28] Wilkinson, P. M., Haringa, H., and Van Dierendonck, L. L., 1994, "Mass transfer and bubble size in a bubble column under pressure," Chem. Eng. Sci., **49**(9), pp. 1417–1427.

[29] Letzel, H. M., Schouten, J. C., Krishna, R., and van den Bleek, C. M., 1999, "Gas holdup and mass transfer in bubble column reactors operated at elevated pressure," Chem. Eng. Sci., **54**(13-14), pp. 2237–2246.

[30] Vandu, C. O., and Krishna, R., 2004, "Influence of scale on the volumetric mass transfer coefficients in bubble columns," Chem. Eng. Process. Process Intensif., **43**(4), pp. 575–579.

[31] Sharqawy, M. H., and Liu, H., 2015, "The effect of pressure on the performance of bubble column dehumidifier," Int. J. Heat Mass Transf., **87**, pp. 212–221.

[32] Liu, H., and Sharqawy, M. H., 2015 (submitted), "Experimental performance of a bubble column humidifier and dehumidifier under varying pressure," Int. J. Heat Mass Transf.

[33] Wu, C., Al-Dahhan, M. H., and Prakash, A., 2007, "Heat transfer coefficients in a high-pressure bubble column," Chem. Eng. Sci., **62**(1-2), pp. 140–147.

[34] Cho, Y. J., Woo, K. J., Kang, Y., and Kim, S. D., 2002, "Dynamic characteristics of heat transfer coefficient in pressurized bubble columns with viscous liquid medium," Chem. Eng. Process. Process Intensif., **41**(8), pp. 699–706.

[35] Lin, T.-J., and Fan, L.-S., 1999, "Heat transfer and bubble characteristics from a nozzle in high-pressure bubble columns," Chem. Eng. Sci., **54**(21), pp. 4853–4859.

[36] Merkel, F., 1925, "Verdunstungskühlung," VDI-Zeitschrift, **70**, pp. 123–128.

[37] Kloppers, J. C., and Kröger, D. G., 2005, "The Lewis factor and its influence on the performance prediction of wet-cooling towers," Int. J. Therm. Sci., **44**(9), pp. 879–884.

[38] Lewis, W. K., 1933, "The evaporation of a liquid into a gas—a correction," Mech. Eng., **55**, pp. 567–573.

[39] Braun, J. E., Klein, S. A., and Mitchell, J. W., 1989, "Effectiveness models for cooling towers and cooling coils," ASHRAE Trans., **95**(2), pp. 164–174.

[40] Miller, D. N., 1974, "Scale-up of agitated vessels gas-liquid mass transfer," AIChE J., **20**(3), pp. 445–453.

[41] Akita, K., and Yoshida, F., 1973, "Gas holdup and volumetric mass transfer coefficient in bubble columns," Ind. Eng. Chem. Process Des. Dev., **12**(1), pp. 76–80.

[42] Shimizu, K., Takada, S., Minekawa, K., and Kawase, Y., 2000, "Phenomenological model for bubble column reactors: prediction of gas hold-ups and volumetric mass transfer coefficients," Chem. Eng. J., **78**(1), pp. 21–28.

[43] Öztürk, S. S., Schumpe, A., and Deckwer, W.-D., 1987, "Organic liquids in a bubble column: Holdups and mass transfer coefficients," AIChE J., **33**(9), pp. 1473–1480.

[44] Hikita, H., Asai, S., Tanigawa, K., Segawa, K., and Kitao, M., 1981, "The volumetric liquid-phase mass transfer coefficient in bubble columns," Chem. Eng. J., **22**(1), pp. 61–69.

[45] Joshi, J. B., and Sharma, M. M., 1979, "A circulation cell model for bubble columns," Chem. Eng. Res. Des., **57a**, pp. 244–251.

[46] Klein, S. A., 2014, "Engineering Equation Solver, Academic Professional V9.698."

[47] Coleman, H. W., and Steele, W. G., 1999, Experimentation and uncertainty analysis for engineers, Wiley, New York.

[48] Calderbank, P. H., and Moo-Young, M. B., 1961, "The continuous phase heat and mass transfer properties of dispersions," Chem. Eng. Sci., **16**(1-2), pp. 39–54.

VITAE

Name	:	Huicheng Liu
Nationality	:	Chinese
Date of Birth	:	6 October, 1989
Email	:	huichgliu@gmail.com
Address	:	Dhahran, Saudi Arabia
Academic Background	:	**Master of Science** in Mechanical Engineering, 2013 - 2015 King Fahd University of Petroleum and Minerals Dhahran, Saudi Arabia **Bachelor of Engineering** in Thermal and Power Engineering, 2008 - 2012 Huazhong University of Science and Technology Wuhan, China **Bachelor of Management** (Minor) in Business Administration, 2010 - 2012 Wuhan University Wuhan, China
Published Paper	:	The effect of pressure on the performance of bubble column dehumidifier, Int. J. Heat Mass Transf., 87 (2015) 212–221.